THE JOURNAL OF BIOLOGICAL CHEMISTRY VOL. 284, NO. 8, pp. 4914–4920, February 20, 2009

Design of Peptide-based Inhibitors for Human Immunodeficiency Virus Type 1 Strains Resistant to T-20*[S]

Received for publication, September 16, 2008, and in revised form, December 3, 2008 Published, JBC Papers in Press, December 10, 2008, DOI 10.1074/jbc.M807169200

Kazuki Izumi[‡], Eiichi Kodama[‡1], Kazuya Shimura[‡], Yasuko Sakagami[‡], Kentaro Watanabe[§], Saori Ito[§], Tsuyoshi Watabe[§], Yukihiro Terakawa[§], Hiroki Nishikawa[§], Stefan G. Sarafianos[¶], Kazuo Kitaura[§], Shinya Oishi[§], Nobutaka Fujii[§], and Masao Matsuoka[‡]

From the [‡]Institute for Virus Research, Kyoto University, 53 Kawaramachi, Shogoin, Kyoto 606-8507, Japan, the [§]Graduate School of Pharmaceutical Sciences, Kyoto University, 46-29 Yoshida, Shimoadachi-cho, Kyoto 606-8501, Japan, and the [¶]Christopher S. Bond Life Sciences Center and Department of Molecular Microbiology and Immunology, University of Missouri School of Medicine, Columbia, Missouri 65211

Enfuvirtide (T-20) is a fusion inhibitor that suppresses replication of human immunodeficiency virus (HIV) variants with multi-drug resistance to reverse transcriptase and protease inhibitors. It is a peptide derived from the C-terminal heptad repeat (C-HR) of HIV-1 gp41, and it prevents interactions between the C-HR and the N-terminal HR (N-HR) of gp41, thus interfering with conformational changes that are required for viral fusion. However, prolonged therapies with T-20 result in the emergence of T-20-resistant strains that contain primary mutations such as N43D in the N-HR of gp41 (where T-20 and C-HR bind) that help the virus escape at a fitness cost. Such variants often go on to acquire a secondary mutation, S138A, in the C-HR of gp41 region that corresponds to the sequence of T-20. We demonstrate here that the role of S138A is to compensate for the impaired fusion kinetics of HIV-1s carrying primary mutations that abrogate binding of T-20. To preempt this escape strategy, we designed a modified T-20 variant containing the S138A substitution and showed that it is a potent inhibitor of both T-20-sensitive and T-20-resistant viruses. Circular dichroism analysis revealed that the S138A provided increased stability of the 6-helix bundle. We validated our approach on another fusion inhibitor, C34. In this case, we designed a variant of C34 with the secondary escape mutation N126K and showed that it can effectively inhibit replication of C34-resistant HIV-1. These results prove that it is possible to design improved peptide-based fusion inhibitors that are efficient against a major mechanism of drug resistance.

HIV-1[2] entry into the target cells is mediated by two envelope glycoproteins, gp120 and gp41, that form a trimeric gp120·gp41 complex. After binding of gp120 to the CD4 receptor and CCR5 (or CXCR4) coreceptor on the surface of the target cell, the gp41 trimer forms an extended conformation of the three helices that allows a hydrophobic fusion peptide to be inserted into the target cell membrane, generating an intermediate that is anchored to both cellular and viral membranes. After this step, the gp41 is believed to start refolding to a more stable 6-helix bundle composed of the α-helical trimer of the N-terminal heptad repeat (N-HR) folded into an anti-parallel conformation with the three C-terminal heptad repeats (C-HR) (1, 2). This refolding brings the viral and cellular membranes together to catalyze fusion.

The transition of the extended intermediate to the 6-helix bundle can be inhibited by the addition of exogenous peptides derived from gp41 C-HR (Fig. 1*A*) that prevent the formation of the 6-helix bundle and inhibit the HIV-1 fusion with the target cells (3–6). T-20, a 36-amino acid peptide derived from C-HR, effectively suppresses *in vivo* replication of HIV-1 resistant to inhibitors of reverse transcriptase and protease (7, 8). However, HIV-1 variants resistant to T-20 have recently emerged carrying primary mutations in the Leu-33–Leu-45 region of the N-HR domain (9–15). Among them, V38A and N43D seem to be major primary mutations for T-20 resistance. Meanwhile, a secondary mutation at the C-HR region (S138A) has been reported to enhance T-20 resistance with an as yet undefined mechanism (9, 14, 15) (Fig. 1*B*).

The mechanism of resistance to C34, another C-HR peptide-based inhibitor of HIV fusion, has been the subject of multiple studies (13, 16). Because of a 22-amino acid overlap between the T-20 and C34 peptides (Fig. 1*B*), HIV-1 has developed primary mutations for C34 resistance *in vitro* at the identical Leu-33–Leu-45 region of the peptides. During *in vitro* selection of C34 resistance, we identified a mutation in the C-HR domain, N126K, that is also observed in some T-20-resistant clinical variants (10, 15, 17). We showed that N126K conferred resistance to C34 by compensating for the impaired intra-gp41 inter-

* This work was supported, in part, by National Institutes of Health Grants AI076119, AI079801, and AI074389 (to S. G. S.). This work was also supported in part by grants from the Ministry of Health and Welfare and the Ministry of Education, Culture, Sports, Science, and Technology of Japan (to E. K., S. O., and N. F.), the Japan Health Sciences Foundation (to E. K., S. O., N. F., and M. M.), the 21st Century COE program (to K. I., S. I., and H. N.), and a Japan Society for the Promotion of Science research fellowship (to H. N.). The costs of publication of this article were defrayed in part by the payment of page charges. This article must therefore be hereby marked "*advertisement*" in accordance with 18 U.S.C. Section 1734 solely to indicate this fact.

[S] The on-line version of this article (available at http://www.jbc.org) contains supplemental Figs. 1 and 2 and Tables 1 and 2.

[1] To whom correspondence should be addressed. Tel. and Fax: 81-75-751-3986; E-mail: ekodama@virus.kyoto-u.ac.jp.

[2] The abbreviations used are: HIV, human immunodeficiency virus; T-20, enfuvirtide; HR, heptad repeat; MAGI, multinuclear activation of galactosidase indicator; EC_{50}, 50% effective concentration; T_m, melting temperature; CD, circular dichroism; shRNA, short hairpin RNA; WT, wild-type.

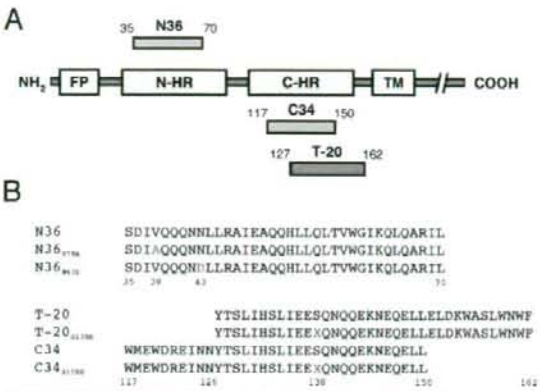

FIGURE 1. **Schematic view of gp41 and peptide sequence.** *A*, structure of HIV-1 gp41 and locations of N-HR or C-HR peptides (*FP*, fusion peptide; *TM*, transmembrane domain). *B*, amino acid sequences of peptides used in this study. Only the amino acid located at Ser-138 was substituted with all physiological amino acids (*X*), as Asn-126 lies outside of the amino acid sequence of T-20.

action by a primary mutation, I37K (13). N126K was initially identified in background of V38A, another primary mutation, for T-20 resistance *in vivo* (17). Baldwin *et al.* (17, 18) demonstrated a striking T-20-dependent replication phenotype in the V38A/N126K variant and proposed that T-20 acts as a safety pin to prevent premature formation of helical bundle, as N126K enhanced binding capacity of the introduced C-HR to N36 with V38A. Taken together, these studies suggest that mutations in the C-HR serve as secondary mutations.

In this study we show that the main role of secondary mutations that follow the appearance of primary mutations during treatment with peptide-based fusion inhibitors is to compensate for the impairment in replication kinetics that is caused by the primary mutations (supplemental Fig. 1). Based on this finding we hypothesized that analogs of T-20 carrying substitutions corresponding to secondary T-20 resistance mutations should be active against both wild-type and T-20-resistant viruses containing primary mutations. Indeed, our results confirmed our hypothesis and showed that T-20 with the S138A substitution ($T\text{-}20_{S138A}$) has a strong anti-HIV-1 activity even against T-20-resistant clones. Moreover, we demonstrate that this restoration is concomitant to improved binding of $C\text{-}HR_{S138A}$ to $N\text{-}HR_{N43D}$, suggesting that our approach utilizing the resistance-associated mutations to design peptides may provide useful broad insights into effective peptide-based therapies.

EXPERIMENTAL PROCEDURES

Cells and Viruses—MT-2 cells were grown in RPMI 1640 medium. 293T cells were grown in Dulbecco's modified Eagle's medium-based culture medium. HeLa-CD4-LTR-β-gal cells were kindly provided by M. Emerman through the AIDS Research and Reference Reagent Program, Division of AIDS, NIAID, National Institutes of Health (Bethesda, MD) and were used for the drug susceptibility assay as described previously (13, 19, 20). An HIV-1 infectious clone, pNL4–3 (21), was used for generation of HIV-1 variants.

Antiviral Agents—The peptides used in this study were synthesized as described previously (6).

Determination of Drug Susceptibility of HIV-1—The peptide sensitivity of infectious clones was determined by the multinuclear activation of galactosidase indicator (MAGI) assay as described previously (13). Briefly, the target cells (HeLa-CD4-LTR-β-gal; 10^4 cells/well) were plated in 96-well flat microtiter culture plates. On the following day the cells were inoculated with the HIV-1 clones (60 MAGI unit/well, giving 60 blue cells after 48 h of incubation) and cultured in the presence of various concentrations of drugs in fresh medium. Forty-eight hours after viral exposure, all the blue cells stained with 5-bromo-4-chloro-3-indolyl-β-D-galactopyranoside (X-gal) were counted in each well. The activity of test compounds was determined as the concentration that blocked HIV-1 replication by 50% (50% effective concentration, (EC_{50}).

Generation of Recombinant HIV-1 Clones—Recombinant infectious HIV-1 clones, carrying various mutations, were generated as described previously (13). Each molecular clone was transfected into 293T cells with *Trans*IT® (Madison, WI). After 48 h, the supernatants were harvested and stored at −80 °C until use.

Circular Dichroism Spectroscopy—Each peptide (10 μM) was mixed with 10 mM phosphate-buffered saline, pH 7.4, and the data were collected using a Jasco spectrometer (Model J-710; Jasco, Tokyo, Japan) equipped with a thermoelectric temperature controller. The thermal stability was assessed by monitoring the change in the circular dichroism signal at 222 nm. The midpoint of the thermal unfolding transition (melting temperature, (T_m) of each complex was determined as described previously (6).

Viral Replication Kinetics Assay—MT-2 cells (10^5 cells/3 ml) were infected with each virus preparation (1000 MAGI unit) for 16 h. The infected cells were then washed and cultured in a final volume of 3 ml. The culture supernatants were harvested after infection on days 2–7, and the levels of p24 antigen were determined (22).

For each competitive HIV-1 replication assay, two infectious clones of interest that had been previously titrated were mixed and added to MT-2 cells (10^5 cells/3 ml) as described previously (13, 22) with minor modifications. To ensure that the two infectious clones being compared were of approximately equal infectivity, a fixed amount (500 MAGI unit) of one infectious clone was mixed with three different amounts (250, 500, and 1000 MAGI unit) of the other infectious clone. On day 1, one-third of the infected MT-2 cells were harvested and washed twice with phosphate-buffered saline, and the cellular DNA was extracted. The purified DNA was subjected to nested PCR and then direct DNA sequencing. The HIV-1 co-culture, which best approximated a 50:50 mixture on day 1, was further propagated. Every 3–4 days, the co-culture supernatant (100 μl) was transmitted to new uninfected MT-2 cells (5×10^5 cells/3 ml). The cells harvested at the end of each passage were subjected to direct sequencing, and the viral population change was determined.

Structure Modeling of gp41 S138A Mutant Core—The gp41 core model was built using the coordinates of crystal structure of the N36/C34 complex (23) (PDB code 1AIK). The coordi-

TABLE 1

Antiviral activity of T-20-derived peptides against T-20-resistant gp41 recombinant viruses

Anti-HIV activity was determined with the MAGI assay. The data shown are the mean values and S.D. that were obtained from the results of at least three independent experiments. Shown in parentheses are the -fold increases in resistance (increase in EC_{50} value) calculated by comparison to a reference virus. Increases of >10-fold are indicated in bold.

	EC_{50}			
	HIV-1_{WT}[a]	HIV-1_{V38A}	HIV-1_{N43D}	HIV-$1_{N43D/S138A}$
	nM			
T-20	2.4 ± 0.6	23 ± 8.2 (9.6)	49 ± 10 (**20**)	84 ± 16 (35)
Small				
$T\text{-}20_{S138G}$	1.3 ± 0.5 (0.5)	65 ± 8.8 (**27**)	141 ± 26 (**59**)	185 ± 68 (**77**)
$T\text{-}20_{S138A}$	0.6 ± 0.1 (0.3)	3.6 ± 1.7 (1.5)	3.5 ± 0.9 (1.5)	3.2 ± 1.0 (1.3)
Hydrophobic				
$T\text{-}20_{S138V}$	0.4 ± 0.2 (0.2)	31 ± 14 (**13**)	22 ± 3.5 (9.2)	23 ± 5.7 (9.6)
$T\text{-}20_{S138L}$	0.7 ± 0.1 (0.3)	13 ± 6 (5.4)	2.9 ± 0.7 (1.2)	2.2 ± 0.4 (0.9)
$T\text{-}20_{S138I}$	0.5 ± 0.1 (0.2)	4.9 ± 2 (2)	2.9 ± 0.8 (1.2)	2.4 ± 0.6 (1)
$T\text{-}20_{S138M}$	0.7 ± 0.2 (0.3)	4.4 ± 0.1 (1.8)	1.7 ± 0.5 (0.7)	1.2 ± 0.4 (0.5)
$T\text{-}20_{S138P}$	446 ± 167 (**186**)	>1000 (>**416**)	>1000 (>**416**)	>1000 (>**416**)
Nucleophilic				
$T\text{-}20_{S138T}$	0.9 ± 0.2 (0.4)	39 ± 8.5 (**16**)	161 ± 35 (**67**)	124 ± 43 (**52**)
Aromatic				
$T\text{-}20_{S138F}$	9.4 ± 2.6 (4)	203 ± 89 (**85**)	393 ± 119 (**164**)	478 ± 116 (**200**)
$T\text{-}20_{S138Y}$	25 ± 9 (**10**)	516 ± 223 (**215**)	>1000 (>**416**)	>1000 (>**416**)
$T\text{-}20_{S138W}$	29 ± 14 (**12**)	>1000 (>**416**)	>1000 (>**416**)	>1000 (>**416**)
Amide				
$T\text{-}20_{S138N}$	19 ± 4 (8)	>1000 (>**416**)	>1000 (>**416**)	>1000 (>**416**)
$T\text{-}20_{S138Q}$	34 ± 11 (**14**)	>1000 (>**416**)	>1000 (>**416**)	>1000 (>**416**)
Acidic				
$T\text{-}20_{S138D}$	210 ± 94 (**88**)	>1000 (>**416**)	>1000 (>**416**)	>1000 (>**416**)
$T\text{-}20_{S138E}$	283 ± 80 (**118**)	>1000 (>**416**)	>1000 (>**416**)	>1000 (>**416**)
Basic				
$T\text{-}20_{S138H}$	210 ± 85 (**88**)	>1000 (>**416**)	>1000 (>**416**)	>1000 (>**416**)
$T\text{-}20_{S138K}$	708 ± 145 (**295**)	>1000 (>**416**)	>1000 (>**416**)	>1000 (>**416**)
$T\text{-}20_{S138R}$	362 ± 114 (**150**)	>1000 (>**416**)	>1000 (>**416**)	>1000 (>**416**)

[a] To improve the replication kinetics, D36G mutation, observed in the majority of HIV-1 strains, was introduced into the NL4-3 background used in this study (reference virus).

nates of the water molecules were removed. Additionally, the hydrogen atoms were placed in optimal positions and refined by the energy minimization with the AMBER9 program (24) using the FF99 force field. Ser-138 in the gp41 core model was replaced with alanine (replacement of -OH with -H), and the positions of the hydrogen atoms were refined as described above. The S138A mutant core model (N36/$C34_{S138A}$ complex) was further optimized by the energy minimization using the FF99 force field with the restraints on each of the three residues of N and C termini and the backbone atoms. The restraint weight was 5.0 kcal/mol $Å^2$.

RESULTS

Effect of Amino Acid Substitutions at 138 on Antiviral Activities—We chemically synthesized peptide analogs of T-20 with all natural amino acid substitutions at the 138 position ($T\text{-}20_{S138X}$) and evaluated them for their ability to inhibit three major T-20-resistant clones using the MAGI assay (13) (Table 1). The results indicated that only $T\text{-}20_{S138A}$ inhibited replication of T-20-resistant clones as efficiently as the wild-type clone. Substitution to glycine enhanced T-20 activity, but unlike $T\text{-}20_{S138A}$, $T\text{-}20_{S138G}$ reduced its activity against T-20-resistant clones by ~2–3-fold as compared with the parental peptide, T-20. Substitutions to hydrophobic amino acids leucine, isoleucine, and methionine maintained their anti-HIV-1 activity; however, those to valine reduced anti-HIV-1 activity to T-20-resistant clones. The proline substitution drastically decreased the anti-HIV-1 activity of the peptide inhibitors.

Nucleophilic amino acid at position 138 of T-20 ($T\text{-}20_{S138T}$) showed similar profiles. Conversely, aromatic and amide substitutions reduced the anti-HIV-1 activity of T-20 against HIV-1_{WT} and T-20-resistant clones. Other amino acid substitutions, especially acidic and basic amino acids, decreased the anti-HIV-1 inhibitory activity even against HIV-1_{WT}. These results suggest that smaller hydrophobic (Ala > Leu, Ile) or more flexible (Met > Thr) residues are preferred in this position. Furthermore, the α-helical structure is important for the interaction, as a mutation to proline which is expected to disrupt the helix (25) resulted in an inactive T-20 analog.

Circular Dichroism—To clarify the mechanism by which the substitutions at Ser-138 influence the antiviral activity of T-20 derivatives, we examined the binding affinities of these peptides to N-HR using circular dichroism (CD) analysis (Fig. 2). CD spectra reveal the presence of stable α-helical structure of the 6-helix bundle that is a requisite for biological activity and is thought to be mechanistically and thermodynamically correlated with HIV-1 fusion (26). Therefore, CD spectra typically at 222 nm indicate interaction of N-HR (N36) and C-HR (T-20 or C34). Because T-20 does not interact significantly *in vitro* with the N36 peptide, which is derived from amino acids 35–70 of N-HR, we used a derivative of C34, a peptide that overlaps with T-20 and also inhibits HIV fusion by the same mechanism. The C34 derivative contained the analogous T-20 substitutions described above (Fig. 1*B*). Consistent with antiviral activities, a mixture of N36 and $C34_{S138P}$ or $C34_{S138W}$ showed no apparent or reduced α-helicity, respectively. For binding with $N36_{V38A}$

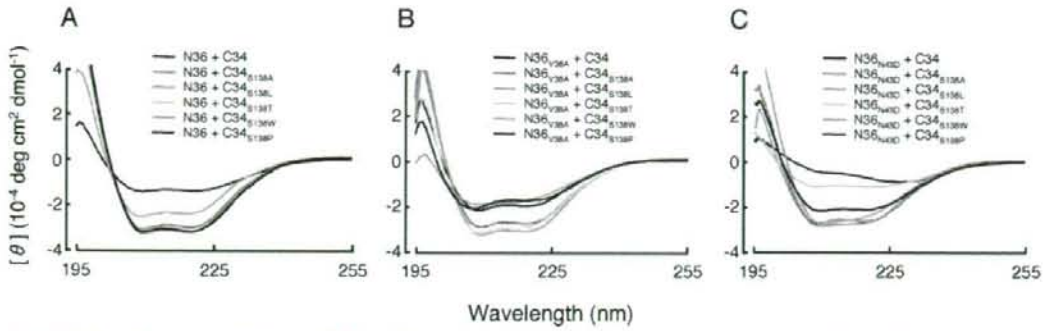

FIGURE 2. **CD spectra of $C34_{S138X}$ complexes with N36 (*A*), $N36_{V38A}$ (*B*), and $N36_{N43D}$ (*C*) are shown.** Equimolar amounts (10 μM) of the N- and C-HR peptides were incubated at 37 °C for 30 min in phosphate-buffered saline. The CD spectra of each mixture were then collected at 25 °C using a Jasco (Model J-710) spectropolarimeter.

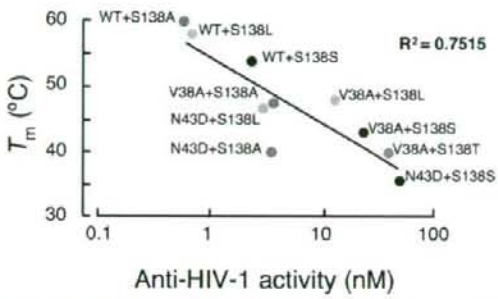

FIGURE 3. **Correlation of T_m values of complexes formed from N36 and C34 peptides (Fig. 2) and anti-HIV-1 activities of $T\text{-}20_{S138X}$ (Table 1).**

or $N36_{N43D}$, sufficient α-helicity at 25 °C was observed only in $C34_{S138A}$, $C34_{S138L}$, and $C34_{S138T}$ or $C34_{S138A}$, $C34_{S138L}$, and $C34_{S138W}$, respectively (Fig. 2, *A–C*).

To determine the thermal stability of the helical complexes formed from the N36 and C34 peptides, we measured the melting temperature (T_m) of each complex (supplemental Table 1). The sigmoidal transition of the CD signal at 222 nm correlates with the thermal stability of the helical complexes formed from the N36 and C34 peptides, which in turn are indicative of the binding affinity of these peptides. The melting temperature (T_m) indicating the 50% disruption of 6-helix bundle was comparatively evaluated. Complexes of N36 and C34 containing the S138A or S138L substitutions ($N36/C34_{S138A}$ or $N36/C34_{S138L}$) showed high thermal stability, comparable with that of the wild-type N36/C34 complex. Similarly, the addition of the S138A or S138L also improved the thermal stability of the $N36_{N43D}$/C34 complex. These results reveal a striking correlation between the thermal stability and the anti-HIV-1 activity of the complexes ($R^2 = 0.75$, Fig. 3). The low T_m value of the complex formed from $N36_{N43D}$ and C34 suggests that virus containing the N43D mutation shows high resistance to T-20, likely due to less favorable thermodynamics that are expected to drive the formation of the 6-helix bundles containing T-20 inhibitor.

Antiviral Activity of Substituted C34 at Ser-138—To confirm that binding of C34 to N-HR is indeed representative of T-20 binding to N-HR, we examined the anti-HIV-1 activities of

TABLE 2

Antiviral activity of $C34_{N126K}$ peptides against C34-resistant gp41 recombinant viruses

Anti-HIV activity was determined by the MAGI assay. The data shown are the mean values and S.D. that were obtained from the results of at least three independent experiments. Shown in parentheses are the -fold increases in resistance (increase in EC_{50} value) calculated by comparison to a reference virus. The increase of >10-fold is indicated in bold.

	EC_{50}	
	$HIV\text{-}1_{WT}$ [a]	$HIV\text{-}1_{\Delta V4/I37K/N126K/L204I}$ [b]
	nM	
C34	1.6 ± 0.35	114 ± 29 (**71**)
$C34_{N126K}$	0.95 ± 0.22 (0.6)	1.1 ± 0.5 (0.7)

[a] To improve the replication kinetics, the D36G mutation, observed in majority of HIV-1 strains, was introduced into the NL4-3 background used in this study (reference virus).

[b] C34-resistant HIV-1 was constructed with the reference virus as described (13). ΔV4 indicates 5 amino acids deletion (FNSTW) in the V4 region of gp120.

C34-derived peptides that have S138A substitutions. The $C34_{S138A}$ and $C34_{S138L}$ peptides showed potent anti-HIV-1 activities, similar to $T\text{-}20_{S138A}$ and $T\text{-}20_{S138L}$ (supplemental Table 2). Based on these findings, we conclude that the stability of complexes comprised of modified C34s and N36s containing T-20 resistance mutations offers a good measure of the binding affinity of $T\text{-}20_{S138X}$ to N-HR.

Antiviral Activity of C34 with N126K—We have recently identified another mutation at the N-HR of gp41 (N126K) during exposure of HIV-1 to C34 *in vitro* (13). The N126K has been occasionally observed after prolonged T-20-containing therapy (10, 15). Here we have confirmed that the $C34_{N126K}$ peptide can also suppress a C34-resistant clone containing several mutations: I37K/N126K/L204I (Table 2). Therefore, peptides designed to have compensatory mutations seem to have potent antiviral activity. However, because residue 126 is located outside the amino acid sequence of T-20 (Fig. 1*B*), we could not examine the effect of N126K substitution on T-20 activity.

Replication Kinetics of Ser-138-substituted HIV-1—To evaluate the effect of Ser-138 substitutions on viral replication, we constructed molecular clones introducing several Ser-138 and determined their replication kinetics by measuring p24 gag antigen production in the culture supernatant. Single nucleotide changes to the TCA codon for Ser-138 may generate 4 amino acid substitutions, Ala, Thr, Leu, Pro, and Trp. As expected, the compensative substitution, S138A, in the T-20

resistance mutation N43D background enhanced replication kinetics of the N43D-containing clone as shown in supplemental Fig. 1. However, in the WT background the S138A appeared to decrease production of p24 as compared with HIV-1_{WT} (Fig. 4). Other substitutions also reduced their replication kinetics. Interestingly, the S138W substitution did not show measurable p24 production. Syncytia induction and single cycle replication kinetics of the Ser-138-substituted HIV-1 were also examined (supplemental Fig. 2). Sizes of syncytia of each virus formed in the MAGI cells (supplemental Fig. 2, *panels A–E*) were associated with p24-normalized single-cycle infectivities (supplemental Fig. 2, *panel F*) and multicycle replication kinetics (Fig. 4). These results suggest that substitutions at Ser-138 are not likely to appear in the absence of T-20 therapy or the emergence of N43D mutation.

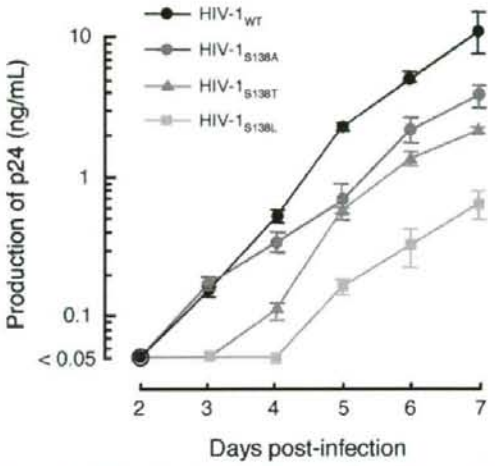

FIGURE 4. **Replication kinetics of HIV-1_{S138X} variants (*X*, any natural amino acid).** HIV-1_{S138A} (*bright red circles*) showed replication kinetics comparable with those seen for HIV-1_{WT} (*blue circles*). Replication of HIV-1_{S138T} (*emerald green triangles*) was reduced, somewhat surprisingly, as both threonine and serine are β-hydroxy amino acids, albeit with different hydrophobicity and torsional flexibility. HIV-1_{S138L} (*orange squares*) also showed reduced replication kinetics. Note that HIV-1_{S138P} and HIV-1_{S138W} failed to replicate (data not shown). Results shown are representative of three independent experiments. An identical order of replication kinetics was observed. Productions of p24 antigen on days 4–7 between HIV-1_{WT} and HIV-1_{S138A} were significant (*t* test, $p < 0.05$).

Structure Modeling—The side chain of amino acid 138 (Ser or Ala) closely contacts with the hydrophobic pocket formed by Leu-44 and Leu-45 in the N-HR. The mutation from Ser to Ala increases hydrophobicity and may help to stabilize the N-HR/C-HR complex related with the potency of the HIV-1 fusion inhibitors (Fig. 5). Larger hydrophobic substitutions such as S138W, S138L, or S138I are likely to sterically interfere with efficient packing of the N-HR and C-HR helices. Similarly, introduction of charged residues at this region of the interface would also disrupt the hydrophobic environment and result in destabilized helix bundles, consistent with the biochemical and virological findings (Figs. 2–4 and Table 1).

Based on crystallographic studies (27, 28), we observe that the T-20 resistance N43D mutation should affect interactions between helices in the 6-helix bundle. Specifically, residue 46 of N-HR is proximal to residue Glu-137 of the C-HR helix of another molecule in the 6-helix bundle. We believe that this increase in proximal negative charges and juxtaposition of Asp-36 next to Glu-137 may destabilize the formation of the 6-helix bundle in a way that results in reduced efficiency of fusion and reduced replication kinetics. Increase of the hydrophobic interactions by introduction of the S138A mutation should help overcome the negative effects of the N43D mutation.

DISCUSSION

In this study we demonstrate that by introducing a secondary resistance mutation into the sequence of peptide-fusion inhibitors such as C34 and T-20, we can suppress efficiently replication of wild-type and of fusion inhibitor-resistant HIV-1. Our circular dichroism analysis revealed that C-HR-based fusion inhibitors that carry secondary resistance mutations can form tight 6-helix bundles with N-HR that contains primary resistance mutations responsible for T-20 resistance. A similar approach has been applied for the development of short hairpin RNA (shRNA) sequences that inhibit HIV-1 replication (29). The synthesized shRNA with mutations that confers resistance to the parental shRNA effectively suppressed replications of shRNA resistant HIV-1 but not wild-type HIV-1. Therefore, it is possible to gain valuable insights from the resistance information and directly apply it to design new peptides or oligonucleotides in the case of shRNA that preempt the viral escape mechanism and suppress resistant variants. Moreover, this strategy should not result in more adverse effect than those that might be obtained during use of the original peptide or oligonucleotide reagents.

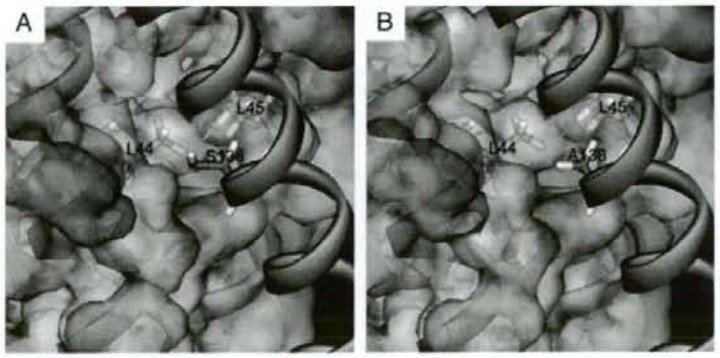

FIGURE 5. **Structure of gp41 at the region near position 138 in the C-HR.** *A*, crystal structure of the N36/C34 complex (PDB code 1AIK). *B*, computational structure modeling of the S138A mutant (N36/$C34_{S138A}$ complex). N-HR and C-HR helices are colored *green* and *orange*, respectively. The van der Waals surface of only N-HR is shown and colored according to the electrostatic potential.

Recently we (6, 30, 31) and others (5) reported that hydrophilic amino

acid substitutions stabilized the α-helix of C-HR peptides and increased their binding affinity to N-HR, thus providing potent anti-HIV activity. This property may be one of the key attributes of the recently developed potent peptide inhibitors, SC34EK (6, 30), T-20EK (31), or T-2429 (5), that have been reported to efficiently inhibit T-20 resistant variants. However, the S138A substitution on T-20 in the present study had little effect on the random coil structure, as judged by CD (data not shown), indicating that $T\text{-}20_{S138A}$ increases its binding affinity not by simply enhancing the α-helicity of this region (5, 6). Our approach of introducing substitutions selected on the basis of the mutation(s) that appears in resistant viruses significantly improved the affinity with N-HR. This approach may complement the effects of enhancing helical stability and may help generate more potent and effective fusion inhibitors for resistant HIV-1 variants.

Other methods have also been employed to improve the potency of HIV fusion inhibitors. For example, T-1249 is a peptide that is based on the T-20 sequence and has improved binding properties (32, 33). It contains 17 changes compared with T-20 (3 additional residues and 14 substitutions to increase the α-helicity/binding affinity according to amino acid sequences of HIV-2 and simian immunodeficiency virus). T-2635 is another efficient peptide fusion inhibitor that was recently developed and is also modified extensively (19 substitutions in 38 amino acids) (5). Also, SC34EK is an electrostatically constrained peptide that also suppresses replication of T-20-resistant variants, and it required 12 substitutions in the original C34 inhibitor (6, 30). Hence, it is possible to improve the potency of existing peptide inhibitors through intense modeling and iterative testing in *in vitro* studies that could lead to the design and synthesis of improved peptide drugs. However, the approach we followed in the design of the $T\text{-}20_{S138A}$ inhibitor is considerably simpler and involves a smaller number of sequence changes (1 residue changed, compared with 19 and 12 in the cases of T-2635 and SC34EK, respectively; see above). It takes advantage of information obtained from the viral evolution under drug pressure and uses the resistance information to design improved inhibitors. In addition, we believe that this approach may be applicable to other targets even when the interactions do not involve helical bundles or detailed information on related systems is not available. Importantly, whenever possible, a combination of the two approaches would likely generate even more effective peptide inhibitors that can suppress replication of resistant variants.

α-Helical structure is a significant factor not only in HIV-1 fusion but also in other examples of protein-protein interactions. Peptide-based drugs have to overcome multiple obstacles, including poor oral bioavailability, less permeability into the target cells, and high cost. Several modifications, such as using arginine-rich peptide tags (34, 35), and chemical treatments (36) have been used to overcome the cell permeability problem. At any rate, peptide-based reagents can be an important tool in the discovery and validation of novel therapeutic targets through *in vitro* experiments. For example, it has been shown that the function of a target protein can be inhibited by designing synthetic peptides that have the amino acid sequence of a domain which is important for the protein function. In such cases the peptides may act as decoys that have antagonistic/agonistic or competitive effects, leading to inhibition of the protein function. Similarly, screening through peptide sequences of proteins may be useful for the identification of functionally important domains that could become future targets for peptide-based or small molecule-based drug development.

In this study we designed peptides tailored to suppress T-20-resistant HIV-1 strains. To our knowledge, this is the first report of direct application of resistance information in drug design and may be applicable to other, unrelated systems. For example, a BH3 domain of the anti-apoptotic protein Bcl-2 has been targeted by an α-helical domain mimic peptide (37, 38). The resulting hydrocarbon-stapled peptide, $SAHB_A$, penetrates into cells via endocytosis pathway and inhibits the function of Bcl-2, inducing apoptosis in transplanted leukemia cells in mice. However, during prolonged therapy with such peptides, leukemic cells could develop resistance to the peptides through substitutions in the Bcl-2 region in the selection process for survival reminiscent of HIV-1. One can envision that our strategy of using mutational resistance information to overcome drug resistance might help in the design of substituted peptides that suppress the resistant variants more efficiently, thus contributing to broader applications of successful peptide-based therapies.

REFERENCES

1. Chan, D. C., and Kim, P. S. (1998) *Cell* **93,** 681–684
2. Weiss, C. D. (2003) *AIDS Rev.* **5,** 214–221
3. Jiang, S., Lin, K., Strick, N., and Neurath, A. R. (1993) *Nature* **365,** 113
4. Chan, D. C., Chutkowski, C. T., and Kim, P. S. (1998) *Proc. Natl. Acad. Sci. U. S. A.* **95,** 15613–15617
5. Dwyer, J. J., Wilson, K. L., Davison, D. K., Freel, S. A., Seedorff, J. E., Wring, S. A., Tvermoes, N. A., Matthews, T. J., Greenberg, M. L., and Delmedico, M. K. (2007) *Proc. Natl. Acad. Sci. U. S. A.* **104,** 12772–12777
6. Otaka, A., Nakamura, M., Nameki, D., Kodama, E., Uchiyama, S., Nakamura, S., Nakano, H., Tamamura, H., Kobayashi, Y., Matsuoka, M., and Fujii, N. (2002) *Angew. Chem. Int. Ed. Engl.* **41,** 2937–2940
7. Lalezari, J. P., Henry, K., O'Hearn, M., Montaner, J. S., Piliero, P. J., Trottier, B., Walmsley, S., Cohen, C., Kuritzkes, D. R., Eron, J. J., Jr., Chung, J., DeMasi, R., Donatacci, L., Drobnes, C., Delehanty, J., and Salgo, M. (2003) *N. Engl. J. Med.* **348,** 2175–2185
8. Lazzarin, A., Clotet, B., Cooper, D., Reynes, J., Arasteh, K., Nelson, M., Katlama, C., Stellbrink, H. J., Delfraissy, J. F., Lange, J., Huson, L., DeMasi, R., Wat, C., Delehanty, J., Drobnes, C., and Salgo, M. (2003) *N. Engl. J. Med.* **348,** 2186–2195
9. Baldwin, C. E., and Berkhout, B. (2006) *Retrovirology* **3,** 84
10. Cabrera, C., Marfil, S., Garcia, E., Martinez-Picado, J., Bonjoch, A., Bofill, M., Moreno, S., Ribera, E., Domingo, P., Clotet, B., and Ruiz, L. (2006) *AIDS* **20,** 2075–2080
11. Labrosse, B., Morand-Joubert, L., Goubard, A., Rochas, S., Labernardiere, J. L., Pacanowski, J., Meynard, J. L., Hance, A. J., Clavel, F., and Mammano, F. (2006) *J. Virol.* **80,** 8807–8819
12. Mink, M., Mosier, S. M., Janumpalli, S., Davison, D., Jin, L., Melby, T., Sista, P., Erickson, J., Lambert, D., Stanfield-Oakley, S. A., Salgo, M., Cammack, N., Matthews, T., and Greenberg, M. L. (2005) *J. Virol.* **79,** 12447–12454
13. Nameki, D., Kodama, E., Ikeuchi, M., Mabuchi, N., Otaka, A., Tamamura, H., Ohno, M., Fujii, N., and Matsuoka, M. (2005) *J. Virol.* **79,** 764–770
14. Perez-Alvarez, L., Carmona, R., Ocampo, A., Asorey, A., Miralles, C., Perez de Castro, S., Pinilla, M., Contreras, G., Taboada, J. A., and Najera, R. (2006) *J. Med. Virol.* **78,** 141–147
15. Xu, L., Pozniak, A., Wildfire, A., Stanfield-Oakley, S. A., Mosier, S. M., Ratcliffe, D., Workman, J., Joall, A., Myers, R., Smit, E., Cane, P. A., Greenberg, M. L., and Pillay, D. (2005) *Antimicrob. Agents Chemother.* **49,**

1113–1119
16. Armand-Ugon, M., Gutierrez, A., Clotet, B., and Este, J. A. (2003) *Antiviral Res.* **59,** 137–142
17. Baldwin, C. E., Sanders, R. W., Deng, Y., Jurriaans, S., Lange, J. M., Lu, M., and Berkhout, B. (2004) *J. Virol.* **78,** 12428–12437
18. Baldwin, C., and Berkhout, B. (2008) *J. Virol.* **82,** 7735–7740
19. Kimpton, J., and Emerman, M. (1992) *J. Virol.* **66,** 2232–2239
20. Maeda, Y., Venzon, D. J., and Mitsuya, H. (1998) *J. Infect. Dis.* **177,** 1207–1213
21. Adachi, A., Gendelman, H. E., Koenig, S., Folks, T., Willey, R., Rabson, A., and Martin, M. A. (1986) *J. Virol.* **59,** 284–291
22. Hachiya, A., Kodama, E. N., Sarafianos, S. G., Schuckmann, M. M., Sakagami, Y., Matsuoka, M., Takiguchi, M., Gatanaga, H., and Oka, S. (2008) *J. Virol.* **82,** 3261–3270
23. Chan, D. C., Fass, D., Berger, J. M., and Kim, P. S. (1997) *Cell* **89,** 263–273
24. Case, D. A., Cheatham, T. E., 3rd, Darden, T., Gohlke, H., Luo, R., Merz, K. M., Jr., Onufriev, A., Simmerling, C., Wang, B., and Woods, R. J. (2005) *J. Comput. Chem.* **26,** 1668–1688
25. Nilsson, I., Saaf, A., Whitley, P., Gafvelin, G., Waller, C., and von Heijne, G. (1998) *J. Mol. Biol.* **284,** 1165–1175
26. Eckert, D. M., and Kim, P. S. (2001) *Annu. Rev. Biochem.* **70,** 777–810
27. Bai, X., Wilson, K. L., Seedorff, J. E., Ahrens, D., Green, J., Davison, D. K., Jin, L., Stanfield-Oakley, S. A., Mosier, S. M., Melby, T. E., Cammack, N., Wang, Z., Greenberg, M. L., and Dwyer, J. J. (2008) *Biochemistry* **47,** 6662–6670
28. Watabe, T., Oishi, S., Watanabe, K., Ohno, H., Nakano, H., Nakatsu, T., Kato, H., Izumi, K., Kodama, E., Matsuoka, M., and Fujii, N. (2009) *Peptide Science*, in press
29. Nishitsuji, H., Kohara, M., Kannagi, M., and Masuda, T. (2006) *J. Virol.* **80,** 7658–7666
30. Nishikawa, H., Nakamura, S., Kodama, E., Ito, S., Kajiwara, K., Izumi, K., Sakagami, Y., Oishi, S., Ohkubo, T., Kobayashi, Y., Otaka, A., Fujii, N., and Matsuoka, M. (September 10, 2008) *Int. J. Biochem. Cell Biol.* 10.1016/j.biocel.2008.08.039
31. Oishi, S., Ito, S., Nishikawa, H., Watanabe, K., Tanaka, M., Ohno, H., Izumi, K., Sakagami, Y., Kodama, E., Matsuoka, M., and Fujii, N. (2008) *J. Med. Chem.* **51,** 388–391
32. Chinnadurai, R., Rajan, D., Munch, J., and Kirchhoff, F. (2007) *J. Virol.* **81,** 6563–6572
33. Eggink, D., Baldwin, C. E., Deng, Y., Langedijk, J. P., Lu, M., Sanders, R. W., and Berkhout, B. (2008) *J. Virol.* **82,** 6678–6688
34. Futaki, S., Suzuki, T., Ohashi, W., Yagami, T., Tanaka, S., Ueda, K., and Sugiura, Y. (2001) *J. Biol. Chem.* **276,** 5836–5840
35. Nagahara, H., Vocero-Akbani, A. M., Snyder, E. L., Ho, A., Latham, D. G., Lissy, N. A., Becker-Hapak, M., Ezhevsky, S. A., and Dowdy, S. F. (1998) *Nat. Med.* **4,** 1449–1452
36. Takeuchi, T., Kosuge, M., Tadokoro, A., Sugiura, Y., Nishi, M., Kawata, M., Sakai, N., Matile, S., and Futaki, S. (2006) *ACS Chem. Biol.* **1,** 299–303
37. Walensky, L. D., Kung, A. L., Escher, I., Malia, T. J., Barbuto, S., Wright, R. D., Wagner, G., Verdine, G. L., and Korsmeyer, S. J. (2004) *Science* **305,** 1466–1470
38. Walensky, L. D., Pitter, K., Morash, J., Oh, K. J., Barbuto, S., Fisher, J., Smith, E., Verdine, G. L., and Korsmeyer, S. J. (2006) *Mol. Cell* **24,** 199–210

ANTIMICROBIAL AGENTS AND CHEMOTHERAPY, Mar. 2009, p. 1013–1018 Vol. 53, No. 3
0066-4804/09/$08.00+0 doi:10.1128/AAC.01211-08

SC29EK, a Peptide Fusion Inhibitor with Enhanced α-Helicity, Inhibits Replication of Human Immunodeficiency Virus Type 1 Mutants Resistant to Enfuvirtide▽

Takeshi Naito,[1] Kazuki Izumi,[1] Eiichi Kodama,[1]* Yasuko Sakagami,[1] Keiko Kajiwara,[1] Hiroki Nishikawa,[2] Kentaro Watanabe,[2] Stefan G. Sarafianos,[3] Shinya Oishi,[2] Nobutaka Fujii,[2] and Masao Matsuoka[1]

Laboratory of Virus Control, Institute for Virus Research, Kyoto University, 53 Kawaramachi, Shogoin, Sakyo-ku, Kyoto 606-8507, Japan[1]; Graduate School of Pharmaceutical Sciences, Kyoto University, Sakyo-ku, Kyoto 606-8501, Japan[2]; and Department of Molecular Microbiology and Immunology, University of Missouri School of Medicine, Columbia, Missouri[3]

Received 12 September 2008/Returned for modification 24 October 2008/Accepted 23 December 2008

Peptides derived from the α-helical domains of human immunodeficiency virus (HIV) type 1 (HIV-1) gp41 inhibit HIV-1 fusion to the cell membrane. Enfuvirtide (T-20) is a peptide-based drug that targets the step of HIV fusion, and as such, it effectively suppresses the replication of HIV-1 strains that are either wild type or resistant to multiple reverse transcriptase and/or protease inhibitors. However, HIV-1 variants with T-20 resistance have emerged; therefore, the development of new and potent inhibitors is urgently needed. We have developed a novel HIV fusion inhibitor, SC34EK, which is a gp41-derived 34-amino-acid peptide with glutamate (E) and lysine (K) substitutions on its solvent-accessible site that stabilize its α-helicity. Importantly, SC34EK effectively inhibits the replication of T-20-resistant HIV-1 strains as well as wild-type HIV-1. In this report, we introduce SC29EK, a 29-amino-acid peptide that is a shorter variant of SC34EK. SC29EK blocked the replication of T-20-resistant HIV-1 strains and maintained antiviral activity even in the presence of high serum concentrations (up to 50%). Circular dichroism analysis revealed that the α-helicity of SC29EK was well maintained, while that of the parental peptide, C29, which showed moderate and reduced inhibition of wild-type and T-20-resistant HIV-1 strains, was lower. Our results show that the α-helicity in a peptide-based fusion inhibitor is a key factor for activity and enables the design of short peptide inhibitors with improved pharmacological properties.

The envelope proteins of human immunodeficiency virus (HIV) type 1 (HIV-1) exist as functional trimeric complexes of gp120-gp41 heterodimers and play an important role in viral entry into host cells. Interactions of gp120 with CD4 molecules expressed on the cell surface cause structural changes that allow further interactions with the CXCR4 or CCR5 coreceptor. These interactions also induce a conformational change in gp120 that initiates gp41-mediated membrane fusion that leads to viral entry (4). In the process of fusion, the amino-terminal heptad repeat (N-HR) of gp41 trimer interacts with the carboxyl-terminal heptad repeat (C-HR) of gp41 trimer to form a six-helix bundle that makes viral and cell membranes accessible (3).

Peptides derived from N-HR or C-HR, such as N36 (3, 18) and enfuvirtide (T-20) (30), suppress the six-helix bundle formation, resulting in the inhibition of membrane fusion. T-20 blocks the entry of various HIV-1 strains, even those resistant to inhibitors of reverse transcriptase and/or protease (15, 16). However, T-20-resistant HIV-1 variants, which frequently show mutations in gp41, such as V38A and N43D, have emerged (14, 25, 26, 28, 32). Therefore, novel fusion inhibitors that suppress the replication of T-20-resistant variants are urgently needed.

C34, a C-HR-derived peptide (Fig. 1A), also inhibits fusion in vitro and does so much more efficiently than T-20 (3, 18, 22). Previously, we remodeled C34 by introducing amino acid substitutions that resulted in highly soluble and active derivatives (24). We replaced amino acids at the solvent-accessible site of the helical bundle with glutamate (E) and lysine (K) and maintained those at the interactive site, as these are critical for the interaction with N-HR. In an α-helical heptad repeat, residues separated by three positions (position i versus position $i + 4$) are located on the same side of the helix and are closely positioned in space (Fig. 1B). Hence, we introduced consecutive EK motifs separated by three residues (E at positions i and $i + 1$ and K at positions $i + 4$ and $i + 5$) of the solvent-accessible site of C34, which resulted in a repeat of the following type: X-EE-XX-KK (where X indicates the original amino acid in HIV-1). A C34 derivative, SC34EK, which has two complete and three incomplete X-EE-XX-KK motifs (Fig. 1), showed enhanced anti-HIV-1 activity compared with that of the parental peptide, C34 (24). A similar result was obtained with T-20EK, the peptide derived by introducing this motif into T-20 (23). Circular dichroism (CD) analysis revealed that both the α-helicity of SC34EK and the thermal stability of the N36-SC34EK complex were enhanced. Interestingly, the antiviral activity of SC35EK, which has five complete X-EE-X X-KK motifs, was comparable to that of SC34EK (24), indicating that five complete X-EE-XX-KK motif repeats are not

* Corresponding author. Mailing address: Laboratory of Virus Control, Institute for Virus Research, Kyoto University, 53 Kawaramachi, Shogoin, Sakyo-ku, Kyoto 606-8507, Japan. Phone and Fax: 81-75-751-3986. E-mail: ekodama@virus.kyoto-u.ac.jp.

▽ Published ahead of print on 29 December 2008.

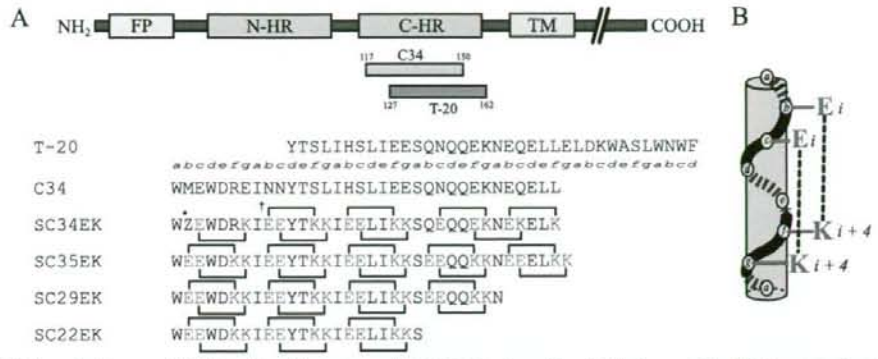

FIG. 1. (A) Schematic diagram of HIV-1 gp41 and sequences of C-HR-derived peptides. FP, fusion peptide; TM, transmembrane domain. The residues at each position in the helical turns are denoted in italics. *Z, an artificial amino acid, norleucine, instead of methionine, to avoid oxidation of the side chain of methionine; †, possible electrostatic interactions indicated by lines and correlating amino acids. (B) One heptad helical turn.

required for strong anti-HIV-1 activity. To address how many complete X-EE-XX-KK motifs are involved in the potent antiviral activity of SC34EK, we synthesized SC29EK and SC22EK (Fig. 1), which contain four and three complete repeats of X-EE-XX-KK, respectively, and evaluated them for their activities against T-20-resistant viruses.

MATERIALS AND METHODS

Cells. HeLa CD4/LTR–β-galactosidase cells obtained from M. Emerman through the AIDS Research and Reference Reagent Program (Germantown, MD) and 293T cells were grown in Dulbecco's modified Eagle medium (DMEM) supplemented with 10% fetal calf serum (FCS), 100 U/ml penicillin G, and 50 μg/ml streptomycin.

Viruses. An HIV-1 infectious clone, pNL4-3 (1), was used for the construction and production of HIV-1 clones. Clones with a certain resistance mutation(s) were introduced by site-directed mutagenesis (29) into the pNL4-3 construct. Although the vast majority of HIV-1 strains have a glycine (G) at position 36 in gp41, the NL4-3 strain used in this study has an aspartic acid (D) residue, which results in impairment of the fusion kinetics of HIV-1 (13, 17). Therefore, in this study, we first constructed a D36G clone, pNL4-3_{D36G}, and used this as a template for the introduction of T-20-resistant mutations, as described previously (21, 31). We constructed three T-20-resistant clones, HIV-$1_{D36G/V38A}$, HIV-$1_{D36G/N43D}$, and HIV-$1_{D36G/N43D/S138A}$ (8), and two C34-resistant clones, HIV-$1_{D36G/N126K}$ and HIV-$1_{\Delta V4/D36G/I37K/N126K/L204I}$ (ΔV4 indicates a five-amino acid [FNSTW] deletion in the V4 region of gp120) (22). Infectious HIV-1 clones were generated by transfection of plasmid clones into 293T cells.

Antiviral agents. Peptide-based fusion inhibitors, including T-20, were synthesized by standard 9-fluorenylmethoxy carbonyl-based solid-phase techniques (24). High-pressure liquid chromatography purification of crude materials on a preparative Cosmosil 5C18 AR-II column with a linear gradient of acetonitrile containing 0.1% trifluoroacetic acid gave the desired peptide samples for biological tests. 2′,3′-Dideoxycytidine (ddC) was purchased from Sigma-Aldrich (St. Louis, MO).

Determination of efficacies of antiviral agents. The efficacies of the antiviral agents were determined by multinuclear activation of galactosidase indicator (MAGI) assays (12, 22). Briefly, 10^4 HeLa CD4/LTR–β-galactosidase cells per well were plated in flat 96-well culture plates. On the following day, the cells were inoculated with the HIV-1 clones (60 MAGI U/well, which gave 60 blue cells after 48 h of incubation) and were cultured in the presence of various concentrations of drugs in fresh medium. After incubation for 48 h after virus inoculation, all of the blue cells that were stained with 5-bromo-4-chloro-3-indolyl-β-D-galactoside in each well were counted. The activities of the test compounds were determined as the concentration that blocked HIV-1 replication by 50% (the 50% effective concentration [EC_{50}]).

Effect of sera on anti-HIV activity. The effect of the FCS concentration on antiviral activity was measured by MAGI assays with FCS at several concentrations (5, 10, 20, and 50%). The effect of serum components on antiviral activity was assessed by MAGI assays. Briefly, T-20 or SC29EK was dissolved in phosphate-buffered saline (PBS), FCS, or serum freshly prepared from HIV-seronegative healthy volunteers at 4 μM; and the mixtures were incubated for 2 h at 37°C. The mixture was diluted to a concentrations of about 1× or 5× the EC_{50} by using a DMEM-based complete medium supplemented with 10% FCS and was subjected to the MAGI assay.

CD analysis. N36- and C-HR-derived peptide complexes were incubated at 37°C for 30 min (final peptide concentration, 10 μM in PBS). The CD spectra were acquired on a spectropolarimeter (model J-710; Jasco Inc., Tokyo, Japan) at 25°C as the average of eight scans. Thermal stability was assessed by monitoring the change in the CD signal at 222 nm as a function of temperature. Thermal unfolding at intervals of 0.5°C was performed after a 15-min equilibration at the desired temperature and an integration time of 1.0 s. The midpoint of the thermal unfolding transition (melting temperature [T_m]) of each complex was determined from the maximum of the first derivative, with respect to the reciprocal of the temperature, of the $[\theta]_{222}$ values.

RESULTS

Antiviral activities of peptides into which EK is introduced. Because W117, W120, and I124, which are crucial for binding to N-HR (2, 3), are located in the N terminus of C34, we deleted the C-terminal region of SC35EK to produce short peptides. SC29EK, which has four complete X-EE-XX-KK motifs, inhibited HIV-1_{NL4-3} infection at a level comparable to that at which SC34EK did (Table 1). As was observed with SC34EK, SC29EK also maintained an inhibitory effect toward T-20-resistant clones. Although SC34EK blocked the replication of C34-resistant clone HIV-$1_{\Delta V4/D36G/I37K/N126K/L204I}$, SC29EK failed to do so. On the other hand, C29, with a 5-amino-acid deletion from the C terminus of C34, exerted drastically reduced antiviral activity. SC22EK, which consisted of three X-EE-XX-KK motifs, also showed much reduced antiviral activity compared with the activities of SC29EK and SC34EK. A native peptide corresponding to SC22EK, C22, exhibited no activity against HIV-1_{NL4-3} at concentrations up to 10 μM (data not shown). Thus, to inhibit the physiological interaction of N-HR and C-HR, a peptide 22 amino acids in length, without modification, may be insufficient. The D36G substitution enhanced the susceptibility of HIV-1 to T-20 (28) but not to C34 or its derivatives (Table 1). These results suggest that four X-EE-XX-KK motifs are required to maintain

TABLE 1. Activities of HIV-1 gp41-derived peptides against T-20-resistant mutants

Virus	EC_{50}[a] (nM)					
	T-20	SC22EK	C29	SC29EK	C34	SC34EK
$HIV\text{-}1_{NL4\text{-}3}$	15 ± 1 (6.3)	217 ± 41 (0.3)	245 ± 42 (4.7)	2.4 ± 0.1 (1.3)	2.3 ± 0.1 (1.0)	1.6 ± 0.2 (0.7)
$HIV\text{-}1_{D36G}$	2.4 ± 0.6	686 ± 94	52 ± 18	1.9 ± 0.0	2.3 ± 0.6	2.4 ± 1.0
$HIV\text{-}1_{D36G/V38A}$	23 ± 8 (9.6)	289 ± 84 (0.4)	504 ± 193 (9.7)	3.0 ± 0.6 (1.6)	4.4 ± 1.4 (1.9)	2.2 ± 0.4 (0.9)
$HIV\text{-}1_{D36G/N43D}$	49 ± 10 (20)	114 ± 36 (0.2)	>1,000 (>19)	4.1 ± 0.6 (2.2)	7.9 ± 0.9 (3.4)	1.6 ± 0.4 (0.7)
$HIV\text{-}1_{D36G/N43D/S138A}$	84 ± 16 (35)	>1,000 (>1.5)	>1,000 (>19)	3.4 ± 0.9 (1.8)	15 ± 2 (6.4)	1.5 ± 0.3 (0.6)
$HIV\text{-}1_{D36G/N126K}$	3.4 ± 0.6 (1.4)	>1,000 (>1.5)	192 ± 22 (3.7)	2.7 ± 0.1 (1.4)	7.0 ± 2.0 (3.0)	12 ± 1 (5.0)
$HIV\text{-}1_{\Delta V4/D36G/I37K/N126K/L204I}$[b]	390 ± 155 (163)	252 ± 71 (0.4)	>1,000 (>19)	50 ± 11 (26)	171 ± 15 (74)	3.0 ± 0.2 (1.3)

[a] Antiviral activity, shown as the EC_{50}, was determined by the MAGI assay. Each EC_{50} represents the mean ± standard deviation obtained from at least three independent experiments. The values in parentheses indicate relative changes (*n*-fold) in the EC_{50} compared with the EC_{50} in the presence of the D36G substitution.
[b] ΔV4 indicates a 5-amino-acid deletion (FNSTW) in the V4 region of gp120.

the inhibitory effect of the peptides on the membrane fusion of HIV-1 strains resistant to T-20, as well as $HIV\text{-}1_{NL4\text{-}3}$.

α-Helicity of the six-helix bundle. To elucidate the mechanism by which SC29EK exerts strong anti-HIV activity, we performed CD analysis of the N36-SC29EK complex. The CD spectrum for the N36-SC29EK complex revealed an α-helix conformation with a characteristic double minimum at 208 nm and 222 nm, similar to the conformations of the N36-C34 and N36-SC35EK complexes. The N36-C29 complex showed an α-helical conformation, while a complex of N36 with C22 showed decreased α-helical spectra (Fig. 2A), in direct correlation to moderately and severely decreased antiviral activities of C29 and C22, respectively. The CD spectra of complexes of N36 peptides containing T-20 resistance-associated mutations with SC29EK, $N36_{V38A}$-SC29EK and $N36_{N43D}$-SC29EK, were almost identical to the CD spectrum of N36 with SC29EK, indicating that SC29EK retains binding affinity for the mutated N36 peptides (Fig. 2B). On the other hand, the mutated N36 peptides and C29 complexes showed little α-helical conformation. These results indicate that introduction of the X-EE-X X-KK motif increases the binding affinity of SC29EK for the mutated N36 peptides.

The thermal stabilities of these complexes were assessed by monitoring the shift in $[\theta]_{222}$ (Fig. 2C). A relatively low T_m (48.5°C) (Fig. 2D) and approximately 80% α-helicity at 37°C (Fig. 2C) were observed with the N36-C29 complex, consistent with its moderate antiviral activity (Table 1). The T_ms of N36- and C-HR-derived peptides into which a X-EE-XX-KK motif was introduced were higher than the T_m of the N36-C34 complex (Fig. 2D), while the T_ms of peptides with the native se-

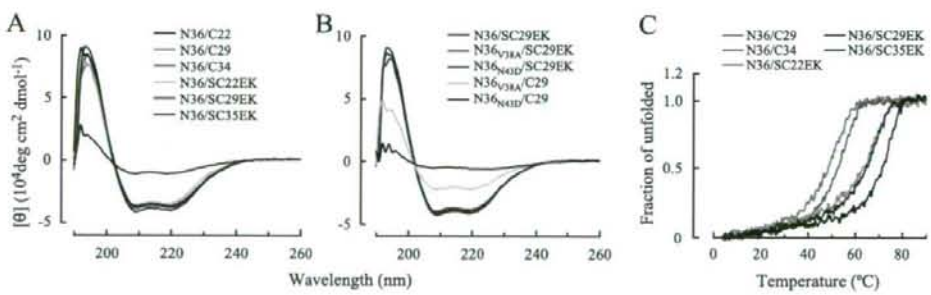

D

peptide		T_m (°C)
N-HR	C-HR	
N36	C29	48.5
N36	C34	52.5
N36	SC22EK	63.5
N36	SC29EK	65
N36	SC35EK	71.5
$N36_{V38A}$	C29	41
$N36_{V38A}$	SC29EK	56
$N36_{N43D}$	C29	NA
$N36_{N43D}$	SC29EK	57

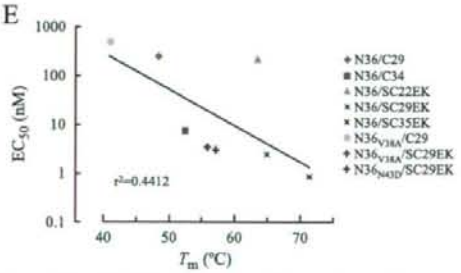

FIG. 2. Analysis of N36 and various C-HR-derived peptides complexes by CD spectroscopy. CD spectra for N36- and C-HR-derived peptide complexes (A) and mutated N36-C29 or SC29EK complexes (B). (C) Temperature-dependent transitions of the dissociation degree of N36 and various C-HR-derived peptide complexes. (D) T_ms of complexes of various N-HR peptides and C-HR peptides. NA, not available. (E) Relation between EC_{50}s of C-HR-derived peptides and T_ms of N36 and various C-HR-derived peptide complexes. The strength of the correlation between EC_{50}s and T_ms is increased ($r^2 = 0.8002$) when the data for SC22EK are excluded.

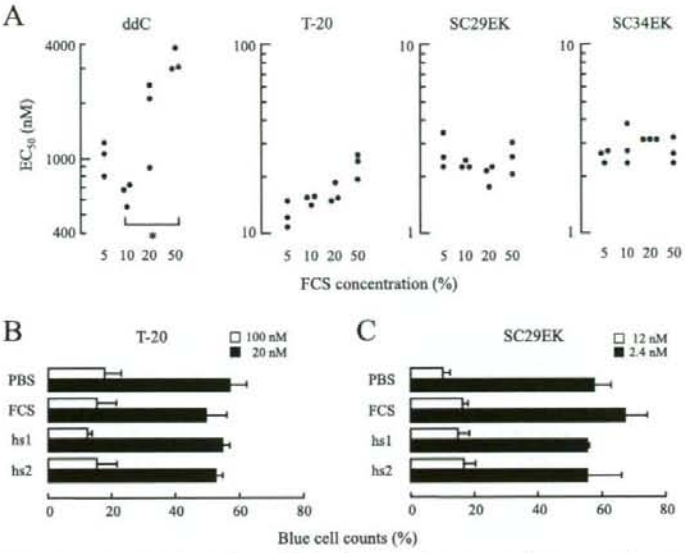

FIG. 3. Effect of serum components on antiviral activity. Antiviral activities in the presence of serum at various concentrations (5, 10, 20, and 50%) were determined by the MAGI assay. (A) Black dots indicate EC_{50}s (nM), each of which was determined three times independently (*, $P = 0.01$ by Student's t test). Antiviral activities of T-20 (B) and SC29EK (C) in human HIV-seronegative sera (hs1 and hs2) were assessed by counting the number of blue cells. Bars indicate the percentages of blue cell counts in PBS, FCS, and human serum compared with the count obtained with no antiviral agents (control, for which the value was 100%). Error bars represent the standard deviation of each mean.

quence but without the introduced motif were lower. The relationships between the EC_{50}s of C-HR-derived peptides and their T_ms are shown in Fig. 2E. The correlation between the EC_{50} and the T_ms was weak ($r^2 = 0.4412$); however, with the exclusion of the data for SC22EK, which showed weak antiviral activity, despite its high T_m, the strength of this correlation was increased ($r^2 = 0.8002$), suggesting that other factors, including solubility and intrapeptide interactions, may be involved in the enhanced antiviral activity of EK-containing peptides.

Effect of serum on antiviral activity. Finally, we assessed the anti-HIV activity of SC29EK in the presence of a high concentration of FCS and in fresh human serum. The activities against HIV-1_{NL4-3} in the presence of various concentrations of FCS (5, 10, 20, and 50%) were determined. A reverse transcriptase inhibitor, ddC, was used as a control. The antiviral activity of ddC was decreased in a concentration-dependent manner (Fig. 3A). In the presence of 50% FCS, the reduction in the EC_{50} of ddC was statistically significant ($P = 0.01$). Similarly, but to a much lesser extent, the EC_{50} of T-20 appeared to be reduced with the FCS concentration in a concentration-dependent manner. Even in the presence of 50% FCS, the mean EC_{50} was comparable to the EC_{50}s in 5% and 10% FCS ($P = 0.082$ and 0.075, respectively). However, the effects of SC29EK and SC34EK were less affected by increased FCS concentrations.

For further evaluation, sera freshly isolated from two HIV-seronegative healthy volunteers were prepared. T-20 and SC29EK incubated for 2 h at 37°C in fresh human serum, FCS, or PBS were diluted with a DMEM-based complete medium supplemented with 10% FCS and were subjected to the MAGI assay. The final FCS concentrations in the various sera that included FCS in these diluted mixtures ranged from 9.75 to 12.2%. Because the antiviral activities of T-20 and SC29EK were not significantly influenced by the FCS concentration (Fig. 3A), it is unlikely that the differences in the FCS concentrations in this experiment had any effect on their antiviral activities. Compared with the inhibitory effects of the PBS-treated peptides, small changes in the inhibitory effects of both T-20 and SC29EK treated with FCS and human sera were observed (Fig. 3B and C). Taken together, these findings suggest that SC29EK stably exerts its strong anti-HIV-1 activity in vivo in the same manner that T-20 does.

DISCUSSION

We show here that SC29EK inhibits the membrane fusion of T-20-resistant HIV-1 strains, suggesting that four X-EE-X X-KK motifs are sufficient to inhibit the fusion of T-20-resistant variants. As revealed by the EC_{50}s and T_ms (Table 1 and Fig. 2), resistance-associated mutations in the N-HR region, such as V38A and N43D, seem to decrease the binding affinity of C-HR-derived peptides for N-HR. Therefore, HIV-1 strains with V38A or N43D show resistance to T-20. However, the anti-HIV-1 activity of SC29EK was less affected by these mutations, because at the physiological temperature for HIV-1 replication, SC29EK showed a stable interaction with N36 peptides containing mutations conferring resistance to T-20. The activity of SC29EK against the C34-resistant clone HIV-$1_{\Delta V4/I336G/I37K/N126K/L204I}$ was decreased, while SC34EK maintained its activity. One of the primary mutations underlying C34 resistance, I37K, is located close to but outside of the

putative binding site of SC29EK. Previously, we reported that an N126K substitution in C-HR enhances the intra-gp41 binding of N-HR and C-HR (22); therefore, we hypothesized that the activity of SC29EK might be decreased by competition with C-HR with the N126K mutation. However, SC29EK also inhibits the entry of HIV-$1_{D36G/N126K}$. Although no structural analysis of the mutated six-helix bundle was performed, it is possible that mutations conferring C34 resistance might induce some structural changes at or adjacent to the SC29EK binding site, because a peptide shortened by a further 7 amino acids, SC22EK, suppressed the entry of the C34-resistant clone.

C34 itself did not have an α-helical spectrum, while SC29EK did (data not shown). SC29EK may achieve its strong antiviral activity by forming an α-helix as a result of E/K substitutions on the solvent-accessible site (Fig. 1). CD analysis shows that HIV-1 builds up resistance to T-20 by introducing certain mutations in N-HR, such as V38A and N43D, which reduce the binding affinity between N-HR and C-HR. SC29EK can efficiently inhibit the fusion of these mutant HIV-1 strains, suggesting that the ability of SC29EK to bind to mutated N-HR and its weak affinity for C-HR are maintained. On the other hand, the D36G, N126K, and S138A mutations increase viral fusion activity (13) by enhancement of the binding affinity of C-HR for N-HR (22, 31). SC29EK effectively suppresses the replication of viruses that have these mutations, such as HIV-1_{D36G}, HIV-$1_{D36G/N43D/S138A}$, and HIV-$1_{D36G/N126K}$. This indicates that the binding capacity of SC29EK is stronger than that of mutated C-HR containing the N126K or the S138A mutation. Therefore, the monomeric α-helical form may inhibit the interactions of N-HR and C-HR with mutations that affect their binding affinity and thus the formation of the six-helix bundle.

Although SC22EK has enhanced α-helicity and a high T_m, it has less antiviral activity than SC29EK. In the interaction between N-HR- and C-HR-derived peptides, while the cavity-forming region (from L54 to Q66) of the C terminus of N-HR (the "pocket") and the cavity-binding region (side chains of W117, W120, and I124) of the N terminus of C-HR (the "knob") play an important role (2, 3, 10), another region of C-HR may also be required. A constrained 14-residue peptide (C14linkmid), which corresponds to the knob region, shows chemical cross-linking and contains amino acid substitutions (27), and it is about 15,000-fold less active than SC29EK, which contains proximal regions in addition to the knob region. These findings also suggest that the knob region of C-HR is important but not sufficient for the formation of a stable complex. Another possible explanation of the weak activity of C14linkmid is that because not only the binding of N-HR and C-HR but also dynamic structural changes are easily anticipated during fusion, it would be difficult to maintain tight binding to the target N-HR due to its rigid constrained form. To maintain the binding of C-HR to N-HR despite such drastic conformational changes during fusion, there may be some unknown interaction, besides the interaction between the pocket and the knob regions, that is necessary for membrane fusion. At present, we cannot conclude whether (i) the length of the peptide itself is crucial, (ii) some other domain has a role, or (iii) a combination of both is important. Further experiments will be needed to clarify the mechanism of inhibition. Such information will be valuable for the generation of effective short peptide inhibitors or small molecules. To generate effective small-molecule inhibitors, if the second possibility is correct, a combination of two agents, one of which interacts with the pocket and the other of which interacts with an unidentified domain, should provide enhanced efficacy. To date, only a limited number of small-molecule compounds that inhibit the six-helix bundle formation with marginal activities have been reported (5, 9, 11), although among the peptide-based inhibitors, several effective peptides have been developed, including T1249 (7), SC34EK (24), T2635 (6), and T-20EK (23).

The T_m of the N36-SC29EK complex was higher than that of the N36-C29 complex, suggesting that EK substitutions reinforced the affinity of binding to N-HR through enhanced α-helicity. It has been considered that the enhanced α-helical structure is maintained by intrahelical salt bridges formed by the introduction of EK substitutions (19). We recently revealed that an electrostatic interaction formed by the EK alignment is involved in enhanced α-helicity (22a), indicating that the strong α-helical stability of SC29EK is probably provided by a mechanism identical to that for SC34EK. Similar peptides with substitutions of glutamate and arginine provided to increase α-helicity have been reported (6). These peptides also increase the stability of the helix and have activity against T-20-resistant HIV-1. Moreover, these peptides were relatively stable in an in vivo model. It is possible that enhanced binding affinity confers nonspecific binding to other α-helical regions of cellular proteins, for example, human serum albumin, which contains 31 α-helical regions (20). However, this effect will be minimal, because the antiviral activity of SC29EK was highly stable in the presence of higher concentrations of FCS and was less affected by human serum.

In this study, we demonstrated that a 29-amino-acid short peptide, SC29EK, suppresses the replication of T-20-resistant variants. SC29EK maintained its activity in the presence of high concentrations of sera, indicating that SC29EK is a candidate short peptide fusion inhibitor.

ACKNOWLEDGMENTS

This work was supported in part by a grant for Research for Health Sciences Focusing on Drug Innovation from the Japan Health Sciences Foundation (E.K., S.O., N.F., M.M.) and a grant for the Promotion of AIDS Research from the Ministry of Health and Welfare of Japan (M.M.). T.N., K.I., and H.N. are supported by the 21st Century COE Program of the Ministry of Education, Culture, Sports, Science, and Technology. S.G.S. was supported by the National Institutes of Health (grants R01AI076119 and 1R21AI079801).

REFERENCES

1. **Adachi, A., H. E. Gendelman, S. Koenig, T. Folks, R. Willey, A. Rabson, and M. A. Martin.** 1986. Production of acquired immunodeficiency syndrome-associated retrovirus in human and nonhuman cells transfected with an infectious molecular clone. J. Virol. **59**:284–291.
2. **Chan, D. C., C. T. Chutkowski, and P. S. Kim.** 1998. Evidence that a prominent cavity in the coiled coil of HIV type 1 gp41 is an attractive drug target. Proc. Natl. Acad. Sci. USA **95**:15613–15617.
3. **Chan, D. C., D. Fass, J. M. Berger, and P. S. Kim.** 1997. Core structure of gp41 from the HIV envelope glycoprotein. Cell **89**:263–273.
4. **Chan, D. C., and P. S. Kim.** 1998. HIV entry and its inhibition. Cell **93**:681–684.
5. **Cianci, C., D. R. Langley, D. D. Dischino, Y. Sun, K. L. Yu, A. Stanley, J. Roach, Z. Li, R. Dalterio, R. Colonno, N. A. Meanwell, and M. Krystal.** 2004. Targeting a binding pocket within the trimer-of-hairpins: small-molecule inhibition of viral fusion. Proc. Natl. Acad. Sci. USA **101**:15046–15051.
6. **Dwyer, J. J., K. L. Wilson, D. K. Davison, S. A. Freel, J. E. Seedorff, S. A. Wring, N. A. Tvermoes, T. J. Matthews, M. L. Greenberg, and M. K. Delmedico.** 2007. Design of helical, oligomeric HIV-1 fusion inhibitor peptides

with potent activity against enfuvirtide-resistant virus. Proc. Natl. Acad. Sci. USA **104:**12772–12777.

7. **Eron, J. J., R. M. Gulick, J. A. Bartlett, T. Merigan, R. Arduino, J. M. Kilby, B. Yangco, A. Diers, C. Drobnes, R. DeMasi, M. Greenberg, T. Melby, C. Raskino, P. Rusnak, Y. Zhang, R. Spence, and G. D. Miralles.** 2004. Short-term safety and antiretroviral activity of T-1249, a second-generation fusion inhibitor of HIV. J. Infect. Dis. **189:**1075–1083.
8. **Fikkert, V., P. Cherepanov, K. Van Laethem, A. Hantson, B. Van Remoortel, C. Pannecouque, E. De Clercq, Z. Debyser, A. M. Vandamme, and M. Witvrouw.** 2002. *env* chimeric virus technology for evaluating human immunodeficiency virus susceptibility to entry inhibitors. Antimicrob. Agents Chemother. **46:**3954–3962.
9. **Frey, G., S. Rits-Volloch, X. Q. Zhang, R. T. Schooley, B. Chen, and S. C. Harrison.** 2006. Small molecules that bind the inner core of gp41 and inhibit HIV envelope-mediated fusion. Proc. Natl. Acad. Sci. USA **103:** 13938–13943.
10. **Ji, H., W. Shu, F. T. Burling, S. Jiang, and M. Lu.** 1999. Inhibition of human immunodeficiency virus type 1 infectivity by the gp41 core: role of a conserved hydrophobic cavity in membrane fusion. J. Virol. **73:**8578–8586.
11. **Jiang, S., H. Lu, S. Liu, Q. Zhao, Y. He, and A. K. Debnath.** 2004. N-substituted pyrrole derivatives as novel human immunodeficiency virus type 1 entry inhibitors that interfere with the gp41 six-helix bundle formation and block virus fusion. Antimicrob. Agents Chemother. **48:**4349–4359.
12. **Kimpton, J., and M. Emerman.** 1992. Detection of replication-competent and pseudotyped human immunodeficiency virus with a sensitive cell line on the basis of activation of an integrated beta-galactosidase gene. J. Virol. **66:**2232–2239.
13. **Kinomoto, M., M. Yokoyama, H. Sato, A. Kojima, T. Kurata, K. Ikuta, T. Sata, and K. Tokunaga.** 2005. Amino acid 36 in the human immunodeficiency virus type 1 gp41 ectodomain controls fusogenic activity: implications for the molecular mechanism of viral escape from a fusion inhibitor. J. Virol. **79:**5996–6004.
14. **Labrosse, B., L. Morand-Joubert, A. Goubard, S. Rochas, J. L. Labernardiere, J. Pacanowski, J. L. Meynard, A. J. Hance, F. Clavel, and F. Mammano.** 2006. Role of the envelope genetic context in the development of enfuvirtide resistance in human immunodeficiency virus type 1-infected patients. J. Virol. **80:**8807–8819.
15. **Lalezari, J. P., K. Henry, M. O'Hearn, J. S. Montaner, P. J. Piliero, B. Trottier, S. Walmsley, C. Cohen, D. R. Kuritzkes, J. J. Eron, Jr., J. Chung, R. DeMasi, L. Donatacci, C. Drobnes, J. Delehanty, and M. Salgo.** 2003. Enfuvirtide, an HIV-1 fusion inhibitor, for drug-resistant HIV infection in North and South America. N. Engl. J. Med. **348:**2175–2185.
16. **Lazzarin, A., B. Clotet, D. Cooper, J. Reynes, K. Arasteh, M. Nelson, C. Katlama, H. J. Stellbrink, J. F. Delfraissy, J. Lange, L. Huson, R. DeMasi, C. Wat, J. Delehanty, C. Drobnes, and M. Salgo.** 2003. Efficacy of enfuvirtide in patients infected with drug-resistant HIV-1 in Europe and Australia. N. Engl. J. Med. **348:**2186–2195.
17. **Lu, J., P. Sista, F. Giguel, M. Greenberg, and D. R. Kuritzkes.** 2004. Relative replicative fitness of human immunodeficiency virus type 1 mutants resistant to enfuvirtide (T-20). J. Virol. **78:**4628–4637.
18. **Lu, M., and P. S. Kim.** 1997. A trimeric structural subdomain of the HIV-1 transmembrane glycoprotein. J. Biomol. Struct. Dyn. **15:**465–471.
19. **Marqusee, S., and R. L. Baldwin.** 1987. Helix stabilization by Glu− . . . Lys+ salt bridges in short peptides of de novo design. Proc. Natl. Acad. Sci. USA **84:**8898–8902.
20. **Matsuo, K., R. Yonehara, and K. Gekko.** 2004. Secondary-structure analysis of proteins by vacuum-ultraviolet circular dichroism spectroscopy. J. Biochem. **135:**405–411.
21. **Mink, M., S. M. Mosier, S. Janumpalli, D. Davison, L. Jin, T. Melby, P. Sista, J. Erickson, D. Lambert, S. A. Stanfield-Oakley, M. Salgo, N. Cammack, T. Matthews, and M. L. Greenberg.** 2005. Impact of human immunodeficiency virus type 1 gp41 amino acid substitutions selected during enfuvirtide treatment on gp41 binding and antiviral potency of enfuvirtide in vitro. J. Virol. **79:**12447–12454.
22. **Nameki, D., E. Kodama, M. Ikeuchi, N. Mabuchi, A. Otaka, H. Tamamura, M. Ohno, N. Fujii, and M. Matsuoka.** 2005. Mutations conferring resistance to human immunodeficiency virus type 1 fusion inhibitors are restricted by gp41 and Rev-responsive element functions. J. Virol. **79:**764–770.

22a. **Nishikawa, H., S. Nakamura, E. Kodama, S. Ito, K. Kajiwara, K. Izumi, Y. Sakagami, S. Oishi, T. Ohkubo, Y. Kobayashi, A. Otaka, N. Fujii, and M. Matsuoka.** Electrostatically constrained alpha-helical peptide inhibits replication of HIV-1 resistant to enfuvirtide. Int. J. Biochem. Cell Biol., in press.

23. **Oishi, S., S. Ito, H. Nishikawa, K. Watanabe, M. Tanaka, H. Ohno, K. Izumi, Y. Sakagami, E. Kodama, M. Matsuoka, and N. Fujii.** 2008. Design of a novel HIV-1 fusion inhibitor that displays a minimal interface for binding affinity. J. Med. Chem. **51:**388–391.
24. **Otaka, A., M. Nakamura, D. Nameki, E. Kodama, S. Uchiyama, S. Nakamura, H. Nakano, H. Tamamura, Y. Kobayashi, M. Matsuoka, and N. Fujii.** 2002. Remodeling of gp41-C34 peptide leads to highly effective inhibitors of the fusion of HIV-1 with target cells. Angew. Chem. Int. Ed. Engl. **41:**2937–2940.
25. **Poveda, E., B. Rodes, C. Toro, L. Martin-Carbonero, J. Gonzalez-Laboz, and V. Soriano.** 2002. Evolution of the gp41 *env* region in HIV-infected patients receiving T-20, a fusion inhibitor. AIDS **16:**1959–1961.
26. **Rimsky, L. T., D. C. Shugars, and T. J. Matthews.** 1998. Determinants of human immunodeficiency virus type 1 resistance to gp41-derived inhibitory peptides. J. Virol. **72:**986–993.
27. **Sia, S. K., P. A. Carr, A. G. Cochran, V. N. Malashkevich, and P. S. Kim.** 2002. Short constrained peptides that inhibit HIV-1 entry. Proc. Natl. Acad. Sci. USA **99:**14664–14669.
28. **Wei, X., J. M. Decker, H. Liu, Z. Zhang, R. B. Arani, J. M. Kilby, M. S. Saag, X. Wu, G. M. Shaw, and J. C. Kappes.** 2002. Emergence of resistant human immunodeficiency virus type 1 in patients receiving fusion inhibitor (T-20) monotherapy. Antimicrob. Agents Chemother. **46:**1896–1905.
29. **Weiner, M. P., G. L. Costa, W. Schoettlin, J. Cline, E. Mathur, and J. C. Bauer.** 1994. Site-directed mutagenesis of double-stranded DNA by the polymerase chain reaction. Gene **151:**119–123.
30. **Wild, C., T. Greenwell, and T. Matthews.** 1993. A synthetic peptide from HIV-1 gp41 is a potent inhibitor of virus-mediated cell-cell fusion. AIDS Res. Hum. Retrovir. **9:**1051–1053.
31. **Xu, L., A. Pozniak, A. Wildfire, S. A. Stanfield-Oakley, S. M. Mosier, D. Ratcliffe, J. Workman, A. Joall, R. Myers, E. Smit, P. A. Cane, M. L. Greenberg, and D. Pillay.** 2005. Emergence and evolution of enfuvirtide resistance following long-term therapy involves heptad repeat 2 mutations within gp41. Antimicrob. Agents Chemother. **49:**1113–1119.
32. **Zollner, B., H. H. Feucht, M. Schroter, P. Schafer, A. Plettenberg, A. Stoehr, and R. Laufs.** 2001. Primary genotypic resistance of HIV-1 to the fusion inhibitor T-20 in long-term infected patients. AIDS **15:**935–936.

Journal of General Virology (2008), 89, 3144–3149 DOI 10.1099/vir.0.2008/004820-0

Short Communication

Substitution of the myristoylation signal of human immunodeficiency virus type 1 Pr55^{Gag} with the phospholipase C-δ1 pleckstrin homology domain results in infectious pseudovirion production

Emiko Urano,[1,2] Toru Aoki,[1] Yuko Futahashi,[1] Tsutomu Murakami,[1] Yuko Morikawa,[2] Naoki Yamamoto[1] and Jun Komano[1]

Correspondence
Jun Komano
ajkomano@nih.go.jp

[1]AIDS Research Center, National Institute of Infectious Diseases, 1-23-1 Toyama, Shinjuku-ku, Tokyo 162-8640, Japan

[2]Kitasato Institute of Life Sciences, Kitasato University, Shirokane 5-9-1, Minato-ku, Tokyo 108-8641, Japan

The matrix domain (MA) of human immunodeficiency virus type 1 Pr55^{Gag} is covalently modified with a myristoyl group that mediates efficient viral production. However, the role of myristoylation, particularly in the viral entry process, remains uninvestigated. This study replaced the myristoylation signal of MA with a well-studied phosphatidylinositol 4,5-biphosphate-binding plasma membrane (PM) targeting motif, the phospholipase C-δ1 pleckstrin homology (PH) domain. PH–Gag–Pol PM targeting and viral production efficiencies were improved compared with Gag–Pol, consistent with the estimated increases in Gag–PM affinity. Both virions were recovered in similar sucrose density-gradient fractions and had similar mature virion morphologies. Importantly, PH–Gag–Pol and Gag–Pol pseudovirions had almost identical infectivity, suggesting a dispensable role for myristoylation in the virus life cycle. PH–Gag–Pol might be useful in separating the myristoylation-dependent processes from the myristoylation-independent processes. This the first report demonstrating infectious pseudovirion production without myristoylated Pr55^{Gag}.

Received 11 June 2008
Accepted 20 August 2008

The N-terminal region [p17^{MA}, matrix (MA) domain] of human immunodeficiency virus type 1 (HIV-1) Pr55^{Gag} (Gag), a structural protein with multiple roles in the virus life cycle (Swanstrom & Wills, 1997), is covalently modified with a myristyol group that aids in plasma membrane (PM) targeting. Removal of this region leads to inefficient Gag targeting to the PM, resulting in dramatically reduced virus production (Bryant & Ratner, 1990; Göttlinger *et al.*, 1989; Pal *et al.*, 1990; Zhou *et al.*, 1994). Although viral particles can be produced by substituting MA with heterologous PM-targeting motifs, such substitution mutants show markedly reduced infectivity (Jouvenet *et al.*, 2006; Scholz *et al.*, 2008), probably due to an active role of MA in viral entry (Kiernan *et al.*, 1998; Wang *et al.*, 1993). However, direct experimental evidence of a viral entry-specific role for MA myristoylation is lacking. Such specific roles of Gag myristoylation can only be determined by separating the myristoylation-dependent PM-targeting function from other MA-associated functions.

We constructed a mutant *gag* expression plasmid where the myristoylated region of Gag was replaced with the N-terminal pleckstrin homology (PH) domain of phospholipase C-δ1 (PLCδ1), a well-studied cellular PM-targeting motif that functions similarly to the myristoyl moiety. PLCδ1 is a member of a family of inositol phospholipid-specific PLC isozymes involved in transducer-mediated intracellular responses (Berridge, 1993). The ~120 aa PH domain can bind to phosphatidylinositol 4,5-biphosphate [PI(4,5)P(2)] and localize to the PM with high affinity and specificity (Ferguson *et al.*, 1995b; Fiorentini *et al.*, 2006; Harlan *et al.*, 1994, 1995; Rhee, 2001; Yagisawa *et al.*, 1994), and green fluorescent protein-bound PLCδ1 PH domains have been used to visualize the PM in living cells (Stauffer *et al.*, 1998; Tall *et al.*, 2000).

We used a codon-optimized HIV-1 *gag–pol* expression vector (p*gag–pol*) for genetic modification of *gag*, as p*gag–pol* increases Gag expression and facilitates protein analyses (Wagner *et al.*, 2000). The substituted mutant retained an intact MA, with the exception of two N-terminal amino acid mutations (ATG→CTG and GGC→GCG), resulting in an MG→LA mutation to knock out the myristoylation signal of Gag and prevent internal translational initiation (Fig. 1a). The PLCδ1 PH domain residues 1–175 (Stauffer *et al.*, 1998) were linked to the LA–Gag N terminus by the amino acids PRAEFT, creating a PH–*gag–pol* expression vector (pPH-*gag-pol*, Fig. 1a). A control PH domain

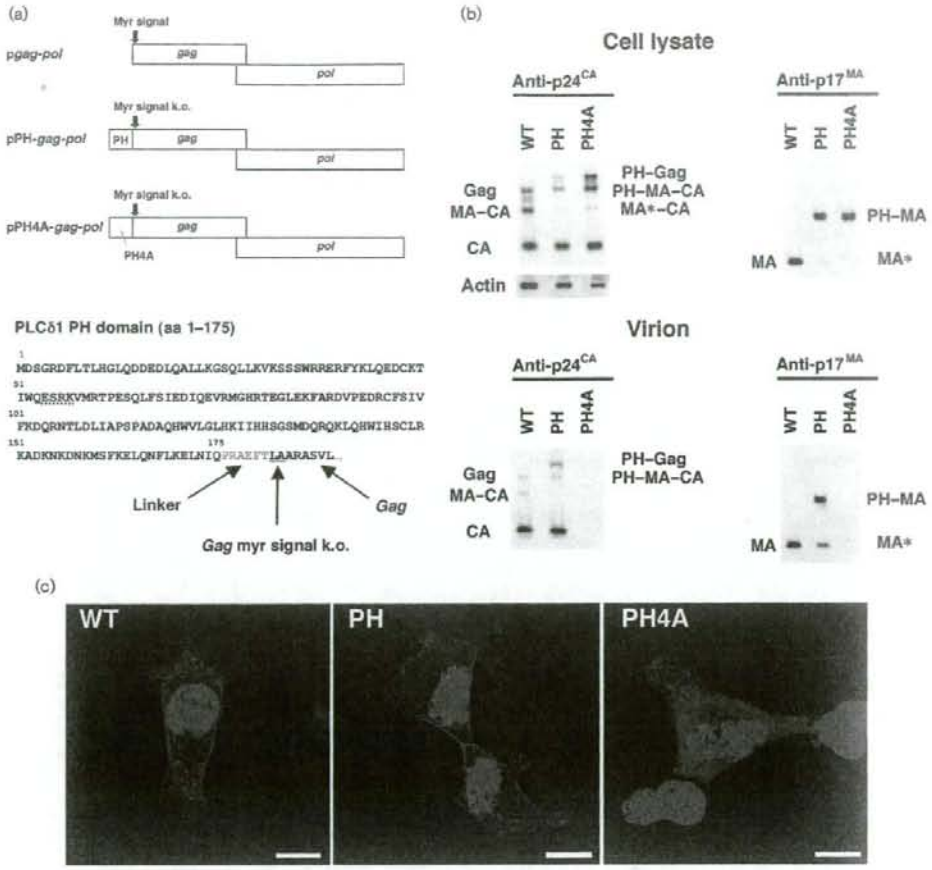

Fig. 1. Viral production by the *gag–pol* expression vectors. (a) The genetic structure of the p*gag-pol*, pPH-*gag-pol* and pPH4A-*gag-pol* expression vectors, and the amino acid sequence of the PH–Gag junction are shown. The N-terminal PH domain of PLCδ1 (aa 1–175) was fused to LA–Gag, linked by a 5 aa spacer (shown in grey). The MG→LA mutation to knock out the myristoylation signal of Gag (myr signal k.o.) is underlined. Four alanine mutations were introduced to replace the ESRK sequence (dotted line) to create the PH4A mutant. (b) Protein expression from p*gag-pol* (WT), pPH-*gag-pol* (PH) and pPH4A-*gag-pol* (PH4A) in transfected 293T cell lysates and Gag cleavage in the virions were examined by Western blot analysis using anti-p24^{CA} or anti-p17^{MA} antibodies. Note that the anti-p17^{MA} antibody recognizes the cleaved p17^{MA} protein only. The band denoted as PH–MA–CA in the virion detected by the anti-p24^{CA} antibody (lower left panel) possibly overlaps with a faint Gag signal derived from PH–Gag and PH4A–Gag from which the PH and PH4A domains have been cleaved. (c) Immunofluorescence assay showing the distribution of Gag, PH–Gag and PH4A–Gag in 293T cells transfected with the respective expression plasmid. Red and blue represent p24^{CA} and the Hoechst 33258-stained nucleus, respectively. Bars, 10 μm.

mutant (PH4A) had mutations at aa 54–57 (ESRK→AAAA; Fig. 1a); these residues are responsible for the PH domain–PI(4,5)P(2) interaction (Ferguson *et al.*, 1995a). PH–Gag, PH4A–Gag and their cleaved products were detected in transfected 293T cell lysates with mouse monoclonal antibodies specific for the p24^{CA} (capsid) domain (anti-p24^{CA}; NIH AIDS Research and Reference Reagent Program) and MA domain (anti-p17^{MA}; Advanced Biotechnologies) (Fig. 1b). PH–Gag cleavage was more efficient than that of Gag, suggesting efficient PM targeting of PH–Gag (Fig. 1b). The Gag protein levels in the pPH4A-*gag-pol*-transfected cell lysate were higher than those in p*gag-pol*- and pPH-*gag-pol*-transfected cell lysates when adjusted for the amount of protein loaded, indicating the low virus-like particle (VLP) production efficiency by PH4A–Gag (Fig. 1b).

The intracellular distribution of Gag, PH–Gag and PH4A–Gag was analysed by immunofluorescence microscopy of transfected 293T cells (Fig. 1c). Transfected cells were grown for 24 h, fixed (4 % formaldehyde), permeabilized (0.1 % Triton X-100 for 5–30 min) and incubated with mouse anti-$p24^{CA}$ and goat anti-mouse antibodies (GE Healthcare Bio-Sciences) conjugated to streptavidin–Alexa Fluor 555 (Invitrogen). Cells were stained with Hoechst 33258, mounted and analysed using confocal microscopy as described previously (Futahashi *et al.*, 2007). Gag was found to be distributed throughout the cytoplasm and at the cell periphery. In contrast, PH–Gag signals were mostly detected at the cell periphery and PH4A–Gag was distributed homogeneously in the cytoplasm. These data clearly showed that PH–Gag targeted the PM more efficiently than Gag, consistent with the Western blot analysis (Fig. 1b). These results also suggested that the efficient PM targeting of PH–Gag depends on the ability of the PH domain to bind PI(4,5)P(2). Similar observations were made in NP2 and COS7 cells.

VLP production was also examined. Tissue culture supernatants of p*gag-pol*-, pPH-*gag-pol*- or pPH4A-*gag-pol*-transfected 293T cells were passed through nitrocellulose filters (0.45 μm) and the virions were collected by centrifugation (541 000 ***g*** for 1 h). Viral antigens, except for PH4A, were detected with anti-$p24^{CA}$ and anti-$p17^{MA}$ antibodies (Fig. 1b). Gag and PH–Gag were further processed by the viral proteases in the virions compared with the cell lysates, as indicated by the increased signals for CA and MA relative to Gag. Interestingly, approximately one-fifth of the PH–Gag in the virion was cleaved close to the PH–MA junction. Presumably, the amino acid sequence at the C end of the PH domain ELQN/FLKE (aa 164–171, where the protease cleaves at the N–F junction) served as a viral protease recognition site as it matched the substrate consensus sequence and resembled the NC–*p1* junction, RQAN/FLGK (de Oliveira *et al.*, 2003; Swanstrom & Wills, 1997). Alternatively, the N terminus of LA–Gag (EFTL/AADS) might be targeted by the viral protease. Thus, the MA released from PH–MA, designated MA*, possibly has 10 aa attached to its N terminus.

The VLP production efficiency was quantified as the concentration of CA in transfected 293T cell culture supernatants relative to that in cell lysates using a p24 ELISA (Zeptometrics). When the CA concentrations of the virion fractions were normalized to those of the cell lysates, the pPH-*gag-pol* viral production efficiency was 3.2-fold higher than that of p*gag-pol* (3.2 ± 2.0-fold, $n=14$, $P<0.001$ by Wilcoxon's matched pairs rank test; representative experiments are shown in Table 1). In contrast, pPH4A-*gag-pol* produced viral particles less efficiently than p*gag-pol* (0.09 ± 0.07-fold, $n=6$, $P<0.05$ by Wilcoxon's matched pairs rank test; representative experiments are shown in Table 1). These data were consistent with the Western blot analysis (Fig. 1b).

To characterize the physical properties of PH–Gag–Pol VLPs, we measured the specific density of virions and examined the virion morphology. Firstly, the VLPs were subjected to 20–70 % (w/w) equilibrium sucrose gradient centrifugation (120 000 ***g*** for 16 h) and fractions were recovered from the bottom to the top. The peak fraction containing the viral CA antigen was determined by p24 ELISA. Gag–Pol and PH–Gag–Pol VLPs were detected in fractions with densities of 1.15 ± 0.01 ($n=5$) and 1.16 ± 0.01 ($n=4$) g ml^{-1}, respectively (not statistically significant; representative experiments are shown in Fig. 2a). Secondly, ultrathin sections of fixed 293T cells (2 % glutaraldehyde, 2 % osmium tetroxide) transfected with p*gag-pol* or pPH-*gag-pol* were imaged by transmission electron microscopy (JEM1200EX at 80 kV or JEM2000EX at 100 kV; JEOL). The PH–Gag–Pol and Gag–Pol VLP

Table 1. Efficiency of virus production from 293T cells transfected with p*gag-pol*, pPH-*gag-pol* or pPH4A-*gag-pol* expression vector

Experiment	Plasmid	$p24^{CA}$ (ng per well)*		Virus production efficiency (B/A)	Fold increase relative to p*gag-pol*
		Cell lysate (A)	Culture supernatant (B)		
1	p*gag-pol*	4 043	4 869	1.204	–
	pPH-*gag-pol*	1 989	8 363	4.206	3.49
	pPH4A-*gag-pol*	3 175	103	0.033	0.03
2	p*gag-pol*	3 521	3 887	1.104	–
	pPH-*gag-pol*	2 638	7 688	2.914	2.64
	pPH4A-*gag-pol*	5 913	1 125	0.190	0.17
3	p*gag-pol*	3 359	4 160	1.239	–
	pPH-*gag-pol*	1 454	5 172	3.558	2.87
	pPH4A-*gag-pol*	4 226	75	0.018	0.01
4	p*gag-pol*	9 666	8 996	0.931	–
	pPH-*gag-pol*	4 699	18 273	3.889	4.18
	pPH4A-*gag-pol*	5 527	534	0.097	0.10

*Cells grown in six-well plates were transfected using Lipofectamine 2000 according to the manufacturer's protocol (Invitrogen).

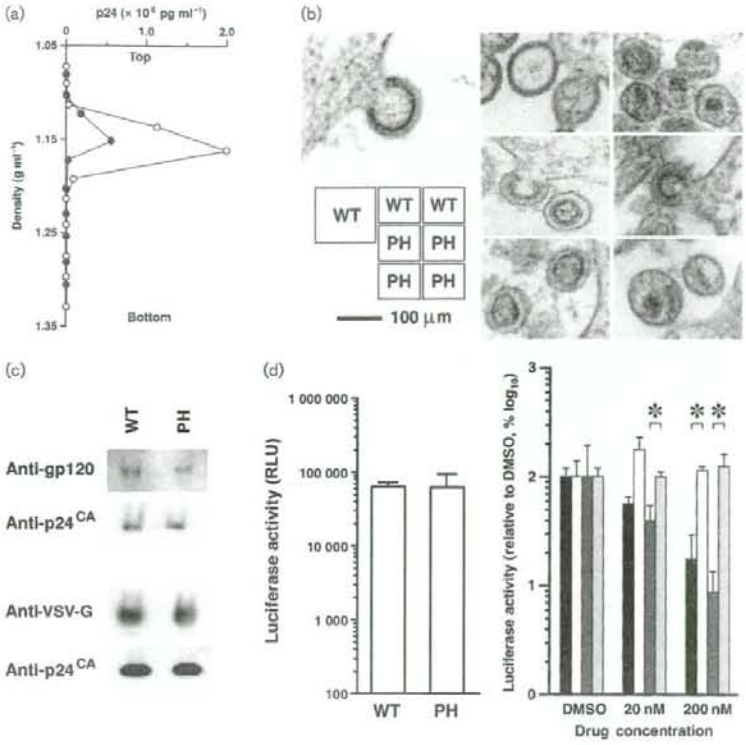

Fig. 2. Physical and biological properties of PH–Gag–Pol VLPs. (a) The virions produced by the p*gag-pol* (WT) and pPH-*gag-pol* (PH) expression vectors were analysed by equilibrium sucrose density-gradient centrifugation. The virion-containing fraction was determined by an ELISA detecting $p24^{CA}$. Representative data from four to five independent experiments are shown. In this experiment, WT (filled circles) and PH (open circles) VLPs migrated in the 1.152 or 1.162 g ml^{-1} density fractions, respectively. (b) Transmission electron microscopy images of 293T cells transfected with p*gag-pol* (WT) or pPH-*gag-pol* (PH). Representative images are shown. (c) Incorporation of HIV-1 Env (upper panel) and VSV-G (lower panel) into Gag–Pol (WT) and PH–Gag–Pol (PH) virions. The virion fractions were subjected to Western blot analysis detecting gp120, VSV-G and $p24^{CA}$. (d) The early phase of the HIV-1 life cycle is supported by PH–Gag–Pol. 293T cells were exposed to virus-containing culture supernatants with similar CA concentrations (270 and 220 ng ml^{-1} for Gag–Pol and PH–Gag–Pol, respectively), and luciferase activities were measured at 2–3 days post-infection as relative light units (RLU). The luciferase activities of PH–Gag–Pol (PH) and Gag–Pol (WT) virus-infected cells were almost identical (left graph). The luciferase transduction by WT (bars 1 and 2) and PH (bars 3 and 4) pseudovirions was performed in the presence of nevirapine (NVP, bars 1 and 3) or TAK-779 (bars 2 and 4). The luciferase signals decreased in the presence of NVP for both WT (bar 1) and PH (bar 3) but not in the presence of TAK-779 for both WT (bar 2) and PH (bar 4), respectively. Representative data from several independent experiments are shown. Asterisks indicate statistical significance ($P<0.01$, $n=3$, Student's *t*-test).

diameters were almost identical (Fig. 2b). Virion budding structures showed that the electron-dense layer, which represented multimerized Gag, of the PH–Gag–Pol VLP was slightly separated from the viral envelope compared with that of the Gag–Pol VLP (Fig. 2b). This indicated that the PH domain was positioned between the viral envelope and the electron-dense layer. In contrast, the morphologies of the mature PH–Gag–Pol and Gag–Pol virions were similar, suggesting that myristoylation is dispensable for mature virion morphology and that the PH–Gag–Pol virion may be infectious.

We examined HIV-1 Env incorporation into the PH–Gag–Pol virion. To do this, we used codon-optimized gp160 (p96ZM651gp160-opt; NIH AIDS Research and Reference Reagent Program). The PH–Gag–Pol virion incorporated HIV-1 Env less efficiently than the Gag–Pol virion as demonstrated by Western blot analysis detecting CA and

gp120 (anti-gp120 antibodies from Santa Cruz Biotechnology; Fig. 2c). This was presumably because PH interfered with the MA–Env interaction. Alternatively, PH may actively incorporate cellular proteins that block efficient Env incorporation into virions. We were unable to evaluate the entry efficacy of PH–Gag–Pol virions pseudotyped by HIV-1 Env because of the limit of detection. PH–Gag–Pol virion infectivity was re-examined by virions pseudotyped with vesicular stomatitis virus G glycoprotein (VSV-G). The incorporation efficiencies of VSV-G into Gag–Pol and PH–Gag–Pol virions were similar (anti-VSV-G antibody from Sigma; Fig. 2c). The lentiviral vector system was used to test this, as HIV-1 provirus gene modifications often fail to produce infectious virions, probably due to viral gene dysregulation. 293T cells were transfected with expression plasmids for Gag–Pol, VSV-G (Komano *et al.*, 2004), Rev and Vpu (a generous gift from Dr H. Göttlinger, University of Massachusetts Medical School, MA, USA), and with a packaging vector encoding a luciferase expression cassette. The HIV-1-based vector expressing firefly luciferase upon infection was recovered 2 days post-transfection. 293T cells were exposed to virus-containing culture supernatants with similar CA concentrations, and luciferase activities were measured at 2–3 days post-infection. When viral preparations with similar p24 concentrations were used, the luciferase activities of PH–Gag–Pol and Gag–Pol virus-infected cells were almost identical to each other (Fig. 2d, left graph). Luciferase expression was blocked by the non-nucleoside reverse transcriptase inhibitor nevirapine (NVP; Boehringer Ingelheim) but not by the CCR5 inhibitor (TAK-779; NIH AIDS Research and Reference Reagent Program), suggesting that gene transduction was mediated by viral infection (Fig. 2d, right panel). Similar results were obtained in several independent experiments. Thus, the PLCδ1 PH domain can functionally replace the HIV-1 Gag myristoylation signal to support both viral production and entry processes, and this myristoylation is dispensable for MA function in the early phase of the virus life cycle. This is the first report describing an infectious pseudovirion without myristoylated Gag. Given that PH–Gag can enhance virus production, HIV-1 with PH–Gag might have been expected to be selected in nature. This is not the case, presumably because the addition of PH to the HIV-1 genome would increase its genome size close to the upper limit that can be incorporated into the retroviral particle, leading to a decrease in genome uptake efficiency, which is clearly a growth disadvantage, despite the enhanced virus production with PH-Gag. More importantly, PH–Gag is unable to incorporate HIV-1 Env efficiently enough to support the production of fully infectious virions. Our data point to the selective advantage of myristoylated Gag in viral evolution.

The myristoylation-dependent Gag–PM association [maximal dissociation constant (K_d) of ~ 0.5–1.0×10^{-5} M] is presumably important for Gag multimerization at the PM (Provitera *et al.*, 2006). After the first contact of Gag with the PM, the membrane binding of Gag is assumed to be stabilized by the Gag–PI(4,5)P(2) interaction (Ono *et al.*, 2004; Saad *et al.*, 2006). The multimerization of Gag appears to induce a conformational change in MA to expose myristoyl groups to enhance the PM targeting of Gag. The higher-order Gag multimerization is probably facilitated by the increased local concentrations of Gag at the PM. Although Gag and PH–Gag are similar to the extent that PI(4,5)P(2) is involved in their PM association, Gag binds to one of the acyl chains of PI(4,5)P(2), as modelled previously (Saad *et al.*, 2006), whilst the PH domain binds the phosphorylated inositol group (Lemmon *et al.*, 1995). The K_d of binding between the PLCδ1 PH domain and PI(4,5)P(2) (~ 1–2×10^{-6} M; Lemmon *et al.*, 1995) suggests that the primary force driving PH–Gag to the PM is at least 2.5-fold stronger than that of myristoylation-mediated PM targeting of Gag. This might be one reason why PH–Gag–Pol was 3.2-fold more efficient at virion production than Gag–Pol. Our data suggest that the myristoyl group-dependent Gag–PM affinity is not a prerequisite for efficient Gag assembly at the PM or for viral production.

The MA has multiple functions throughout the virus life cycle (reviewed by Bukrinskaya, 2007; Fiorentini *et al.*, 2006; Hearps & Jans, 2007; Klein *et al.*, 2007). In the PH–Gag–Pol virion, approximately one-fifth of the PH–MA was unanchored from the PM as MA* (Fig. 1b), which might accompany the pre-integration complex to support nuclear targeting. Using PH–Gag–Pol might enable separation of myristoylation-dependent and -independent MA functions, particularly during the entry phase. PH–Gag–Pol might also be useful for producing high-titre lentiviral vectors or for studying Gag trafficking in cells that poorly support PM targeting of myristoylated Gag, such as rodent cells. Furthermore, functional assays comparing the virus production of Gag–Pol and PH–Gag–Pol might enable the identification of chemical inhibitors or cellular factors specifically targeting myristoylated Gag.

Acknowledgements

We thank Dr H. Göttlinger for critically reading the manuscript. This work was supported by the Japan Health Science Foundation, the Japanese Ministry of Health, Labor and Welfare (H18-AIDS-W-003) and the Japanese Ministry of Education, Culture, Sports, Science and Technology (18689014 and 18659136).

References

Berridge, M. J. (1993). Inositol trisphosphate and calcium signalling. *Nature* **361**, 315–325.

Bryant, M. & Ratner, L. (1990). Myristoylation-dependent replication and assembly of human immunodeficiency virus 1. *Proc Natl Acad Sci U S A* **87**, 523–527.

Bukrinskaya, A. (2007). HIV-1 matrix protein: a mysterious regulator of the viral life cycle. *Virus Res* **124**, 1–11.

de Oliveira, T., Engelbrecht, S., Janse van Rensburg, E., Gordon, M., Bishop, K., zur Megede, J., Barnett, S. W. & Cassol, S. (2003). Variability at human immunodeficiency virus type 1 subtype C protease cleavage sites: an indication of viral fitness? *J Virol* **77**, 9422–9430.

Ferguson, K. M., Lemmon, M. A., Schlessinger, J. & Sigler, P. B. (1995a). Structure of the high affinity complex of inositol trisphosphate with a phospholipase C pleckstrin homology domain. *Cell* **83**, 1037–1046.

Ferguson, K. M., Lemmon, M. A., Sigler, P. B. & Schlessinger, J. (1995b). Scratching the surface with the PH domain. *Nat Struct Biol* **2**, 715–718.

Fiorentini, S., Marini, E., Caracciolo, S. & Caruso, A. (2006). Functions of the HIV-1 matrix protein p17. *New Microbiol* **29**, 1–10.

Futahashi, Y., Komano, J., Urano, E., Aoki, T., Hamatake, M., Miyauchi, K., Yoshida, T., Koyanagi, Y., Matsuda, Z. & Yamamoto, N. (2007). Separate elements are required for ligand-dependent and -independent internalization of metastatic potentiator CXCR4. *Cancer Sci* **98**, 373–379.

Göttlinger, H. G., Sodroski, J. G. & Haseltine, W. A. (1989). Role of capsid precursor processing and myristoylation in morphogenesis and infectivity of human immunodeficiency virus type 1. *Proc Natl Acad Sci U S A* **86**, 5781–5785.

Harlan, J. E., Hajduk, P. J., Yoon, H. S. & Fesik, S. W. (1994). Pleckstrin homology domains bind to phosphatidylinositol-4,5-bisphosphate. *Nature* **371**, 168–170.

Harlan, J. E., Yoon, H. S., Hajduk, P. J. & Fesik, S. W. (1995). Structural characterization of the interaction between a pleckstrin homology domain and phosphatidylinositol 4,5-bisphosphate. *Biochemistry* **34**, 9859–9864.

Hearps, A. C. & Jans, D. A. (2007). Regulating the functions of the HIV-1 matrix protein. *AIDS Res Hum Retroviruses* **23**, 341–346.

Jouvenet, N., Neil, S. J., Bess, C., Johnson, M. C., Virgen, C. A., Simon, S. M. & Bieniasz, P. D. (2006). Plasma membrane is the site of productive HIV-1 particle assembly. *PLoS Biol* **4**, e435.

Kiernan, R. E., Ono, A., Englund, G. & Freed, E. O. (1998). Role of matrix in an early postentry step in the human immunodeficiency virus type 1 life cycle. *J Virol* **72**, 4116–4126.

Klein, K. C., Reed, J. C. & Lingappa, J. R. (2007). Intracellular destinies: degradation, targeting, assembly, and endocytosis of HIV Gag. *AIDS Rev* **9**, 150–161.

Komano, J., Miyauchi, K., Matsuda, Z. & Yamamoto, N. (2004). Inhibiting the Arp2/3 complex limits infection of both intracellular mature vaccinia virus and primate lentiviruses. *Mol Biol Cell* **15**, 5197–5207.

Lemmon, M. A., Ferguson, K. M., O'Brien, R., Sigler, P. B. & Schlessinger, J. (1995). Specific and high-affinity binding of inositol phosphates to an isolated pleckstrin homology domain. *Proc Natl Acad Sci U S A* **92**, 10472–10476.

Ono, A., Ablan, S. D., Lockett, S. J., Nagashima, K. & Freed, E. O. (2004). Phosphatidylinositol (4,5) bisphosphate regulates HIV-1 Gag targeting to the plasma membrane. *Proc Natl Acad Sci U S A* **101**, 14889–14894.

Pal, R., Reitz, M. S., Jr, Tschachler, E., Gallo, R. C., Sarngadharan, M. G. & Veronese, F. D. (1990). Myristoylation of gag proteins of HIV-1 plays an important role in virus assembly. *AIDS Res Hum Retroviruses* **6**, 721–730.

Provitera, P., El-Maghrabi, R. & Scarlata, S. (2006). The effect of HIV-1 Gag myristoylation on membrane binding. *Biophys Chem* **119**, 23–32.

Rhee, S. G. (2001). Regulation of phosphoinositide-specific phospholipase C. *Annu Rev Biochem* **70**, 281–312.

Saad, J. S., Miller, J., Tai, J., Kim, A., Ghanam, R. H. & Summers, M. F. (2006). Structural basis for targeting HIV-1 Gag proteins to the plasma membrane for virus assembly. *Proc Natl Acad Sci U S A* **103**, 11364–11369.

Scholz, I., Still, A., Dhenub, T. C., Coday, K., Webb, M. & Barklis, E. (2008). Analysis of human immunodeficiency virus matrix domain replacements. *Virology* **371**, 322–335.

Stauffer, T. P., Ahn, S. & Meyer, T. (1998). Receptor-induced transient reduction in plasma membrane PtdIns(4,5)P2 concentration monitored in living cells. *Curr Biol* **8**, 343–346.

Swanstrom, R. & Wills, J. W. (1997). Synthesis, assembly, and processing of viral proteins. In *Retroviruses*, pp. 263–334. Edited by J. M. Coffin, S. H. Hughes & H. Varmus. Cold Spring Harbor: Cold Spring Harbor Laboratory Press.

Tall, E. G., Spector, I., Pentyala, S. N., Bitter, I. & Rebecchi, M. J. (2000). Dynamics of phosphatidylinositol 4,5-bisphosphate in actin-rich structures. *Curr Biol* **10**, 743–746.

Wagner, R., Graf, M., Bieler, K., Wolf, H., Grunwald, T., Foley, P. & Uberla, K. (2000). Rev-independent expression of synthetic *gag-pol* genes of human immunodeficiency virus type 1 and simian immunodeficiency virus: implications for the safety of lentiviral vectors. *Hum Gene Ther* **11**, 2403–2413.

Wang, C. T., Zhang, Y., McDermott, J. & Barklis, E. (1993). Conditional infectivity of a human immunodeficiency virus matrix domain deletion mutant. *J Virol* **67**, 7067–7076.

Yagisawa, H., Hirata, M., Kanematsu, T., Watanabe, Y., Ozaki, S., Sakuma, K., Tanaka, H., Yabuta, N., Kamata, H. & other authors (1994). Expression and characterization of an inositol 1,4,5-trisphosphate binding domain of phosphatidylinositol-specific phospholipase C-δ1. *J Biol Chem* **269**, 20179–20188.

Zhou, W., Parent, L. J., Wills, J. W. & Resh, M. D. (1994). Identification of a membrane-binding domain within the amino-terminal region of human immunodeficiency virus type 1 Gag protein which interacts with acidic phospholipids. *J Virol* **68**, 2556–2569.

Efficient inhibition of SDF-1α-mediated chemotaxis and HIV-1 infection by novel CXCR4 antagonists

Yuki Iwasaki,[1] Hirofumi Akari,[1,4] Tsutomu Murakami,[2] Sei Kumakura,[3] Md. Zahidunnabi Dewan,[2,5] Mikiro Yanaka[3,6] and Naoki Yamamoto[2]

[1]Laboratory of Disease Control, Tsukuba Primate Research Center, National Institute of Biomedical Innovation, Tsukuba; [2]AIDS Research Center, National Institute of Infectious Diseases, Tokyo; [3]Biomedical Research Laboratories, Kureha Corporation, Tokyo, Japan

(Received November 11, 2008/Revised December 25, 2008/Accepted December 25, 2008)

CXC chemokine receptor-4, the receptor for stromal cell-derived factor-1α as well as human immunodeficiency virus type 1, belongs to the chemokine receptor family and has been shown to play a critical role in directing the migration of cancer cells to sites of metastasis as well as human immunodeficiency virus type 1 infection. We had previously reported that a duodenally absorbable CXC chemokine receptor-4 antagonist, KRH-1636, showed a potent anti-human immunodeficiency virus type 1 activity both *in vivo* and *in vitro*. In this study, we initially examined the effect of the compound and its derivatives on stromal cell-derived factor-1α-mediated chemotaxis of cancer cells in order to evaluate if they could be applicable as a novel inhibitor of cancer metastasis. We found that both KRH-2731 and KRH-3955 were highly potent antagonists of stromal cell-derived factor-1α-mediated chemotaxis, i.e. the derivatives exhibited 50% effective concentrations of less than 10 nM, for more than 1000-fold efficacy improvement over the prototype KRH-1636. We further demonstrated the greater anti-human immunodeficiency virus type 1 efficacy of the derivatives compared with the original KRH-1636. Taken together, the KRH-1636 derivatives KRH-2731 and KRH-3955 may be promising as a novel inhibitory drug for cancer metastasis as well as for human immunodeficiency virus type 1 infection. (*Cancer Sci* 2009)

Chemokines are secretory proteins with a molecular weight of about 8–14 kDa, and are generally alkaline and heparin-bound. The small chemokine proteins are classified into four highly conserved groups, i.e. CXC, CC, C, and CX3C (X indicates the number of amino acids between the cysteine residues) on the basis of the position of the first two cysteines that are adjacent to the amino terminus.[1] An established role for several members of the CXC and CC chemokine families is to provide directional cues for the movement of leukocytes in development, homeostasis, and inflammation.[2] At the time of the movement of leukocytes, chemokine concentration gradually increases at the inflammatory site because the chemoattractants released from the luminal surface of the endothelium, the inflammatory site of the lymphocyte, are rapidly diluted and swept downstream by blood flow. Leukocytes in the mainstream of blood flow may make contact with the endothelium via a group of molecules called selectins,[3] and may then roll along the endothelial surface.

The cell surface molecule CXC chemokine receptor-4 (CXCR4) is a 7-transmembrane-spanning, G-protein-coupled receptor for the CXC chemokine stromal cell-derived factor-1α (SDF-1α)/pre-B-cell growth stimulating factor (PBSF)/CXCL12.[2] The open reading frame of the *CXCR4* gene encodes a peptide of 352 amino acids and is interrupted by one intron in the region encoding the N-terminal segment.[4]

CXCR4 is a receptor for the SDF-1α. SDF-1α interacts with CXCR4 to play a variety of physiological roles: B-cell formation in liver and bone marrow at the fetal stage, homing of bone marrow cells in the developmental process, formation of the interventricular septum, regulation of movement of the cerebellum granule cell in neurogenesis, and large vasculogenesis that nourishes the gastrointestinal tract.[2] Since both CXCR4 and SDF-1α knockout mice do not survive, the interaction between these molecules is essential in the developmental process.[5–7] It has been reported recently that CXCR7 binds with high affinity to SDF-1α and to interferon-inducible T-cell α-chemoattractant (I-TAC, also known as CXCL11).[8] However, unlike other chemokine receptors, ligand activation of CXCR7 induces neither Ca^{2+} mobilization nor cell migration.[8]

CXCR4 is also shown to be one of the coreceptors for human immunodeficiency virus type 1 (HIV-1).[9] Entry of HIV-1 into target cells involves interactions of the viral envelope protein (Env) with CD4 and a coreceptor, mainly either CXCR4 for T-cell–tropic HIV-1,[10,11] or CCR5 for macrophage–tropic HIV-1.[12,13] In acute HIV-1 infection, primarily macrophage-tropic strains are involved in transmission of the virus, whereas T-cell–tropic strains emerge later and are associated with the rapid progression to AIDS.[9]

Importantly, cancer cells originating from the pancreas, brain, breast, prostate, kidney, ovaries, thyroid, and malignant melanoma express CXCR4; however, normal tissues scarcely express CXCR4. Increasing CXCR4 promotes metastasis of these tumor cells toward SDF-1α-expressing organs including the lungs, liver, lymph nodes, bone marrow, and adrenal glands.[14–17] Further, interaction between CXCR4 and SDF-1α promotes progression of chronic and acute lymphocytic leukemia,[3] and exacerbation of chronic rheumatoid arthritis.[18]

We previously reported that a duodenally absorbable CXCR4 antagonist, KRH-1636, competitively blocked the association of the Env protein of HIV-1 with CXCR4 both *in vivo* and *in vitro* as well as the interaction of SDF-1α with CXCR4.[19] We therefore hypothesized that KRH-1636 could be a promising chemical for offering protection from both cancer metastases induced by SDF-1α and from CXCR4-tropic HIV-1 infection. In order to assess this possibility, we sought to evaluate whether the CXCR4 antagonist KRH-1636 and its derivatives could potently inhibit SDF-1α-mediated chemotaxis of cancer cells as well as HIV-1 infection.

Materials and Methods

Reagents. SDF-1α (R&D systems, Minneapolis, MN, USA) was dissolved in phosphate-buffered saline (PBS) at 1 μM. KRH-1636,[19] and its derivatives KRH-2731, -3148, and -3955 were synthesized at Kureha Chemical Industry (Tokyo, Japan). These

[4]To whom correspondence should be addressed. E-mail: akari@nibio.go.jp
[5]Current address: Department of Pathology, New York University School of Medicine, 550 First Avenue, New York, NY 10016, USA.
[6]Current address: Kureha Special Laboratory Co. Ltd. Fukushima 974-8232, Japan

Abbreviations: CXCR4, CXC chemokine receptor-4; DMSO, dimetyl sulfoxide; EC_{50}, 50% effective concentration; Env, envelope protein; FACS, fluorescence-activated cell sorter; FCS, fetal calf serum; HIV-1, human immunodeficiency virus type 1; mAb, monoclonal antibody; OD, optical density; PBS, phosphate-buffered saline; PBSF, pre-B-cell growth stimulating factor; PE, phycoerythrin; SDF-1α, stromal cell derived factor-1α.

doi: 10.1111/j.1349-7006.2009.01104.x